



Network of European Research Infrastructures for Earthquake Risk Assessment and Mitigation

Report

Guidelines for optimal design of force vibration method

Activity:	<i>COORD</i>
Activity number:	<i>NA6: Networking Field Testing Infrastructures – Task 6.3</i>
Deliverable:	<i>Guidelines for optimal design of force vibration method</i>
Deliverable number:	<i>D6.3</i>
Responsible activity leader:	<i>AIT</i>
Responsible participant:	<i>AUTH, KU LEUVEN</i>
Author:	<i>AIT</i>

Seventh Framework Programme
EC project number: 262330



Deliverable Contributors

AIT – Austrian Institute of Technology	Mariantonietta Morga
AUTH – Laboratory of Geotechnical Earthquake Engineering of the Department of Civil Engineering of Aristotle University of Thessaloniki	Dimitris Pitilakis Maria Manakou
EUCENTRE – European Centre for Training and Research in Earthquake Engineering	Simone Peloso
KUL – Katholieke Universiteit Leuven	Guido De Roeck TienThanh Bui

Within this workpackage 2 additional deliverables were produced:

D6.4 - Testing vulnerability analysis with the European building inventory: a pilot experiment.

D6.5 - NERA workshop "Field testing and seismic vulnerability assessment", Vienna, 25 - 26 September 2014.

All deliverables are available from the NERA repository at ORFEUS:

<http://www.orfeus-eu.org/organization/projects/NERA>

1 Table of Contents

1	Table of Contents	3
2	Introduction.....	8
2.1	Forced vs. ambient vibration testing.....	8
3	Mathematical treatise on forced excitation	9
3.1	Forced vibration applied to a single storey building.....	9
3.2	Forced vibrations applied to multistorey buildings	13
3.3	Response to harmonic excitation.....	15
3.4	Excitation Signals.....	16
4	Methods of structural excitation.....	18
4.1	Excitation devices	18
4.1.1	Inertial shakers	19
4.1.2	Electrohydraulic shakers	20
4.1.3	Electromagnetic shakers	20
4.1.4	Impact hammers	21
4.1.5	Pull and release methods	22
4.1.6	Other excitation mechanisms	23
5	Methodology	23
5.1	Test planning	23
5.2	Instrumentation.....	24
5.3	Data acquisition board	24
5.4	Data acquisition boards for forced vibration methods.....	26
5.5	Types of sensors	26
5.6	Attachment to the structure	28
5.7	Positioning of the exciter.....	31
5.8	Shaker selection	32
6	Data processing and interpretation	32
6.1	Quality control and data filtering	32
6.2	Determination of dynamic characteristics	36
6.2.1	System identification.....	37
6.2.2	Deriving modal parameters	39
6.3	Interpretation methods.....	40
6.3.1	Finite element (FE) model updating.....	40
6.3.2	Derivation of fragility curves based on experimental modal parameters	40
7	Soil-structure interaction	42
7.1	Introduction	42
7.2	Instrumentation scheme	42

7.3	Experimental campaign	45
7.4	Ambient noise measurements.....	45
7.5	Forced-vibration measurements.....	49
7.6	Remarks	56
7.7	Acknowledgements	57
8	Concluding remarks	57
9	Case studies on forced vibration testing.....	58
9.1	Industrial building (Seibersdorf, Austria).....	58
9.1.1	Field testing	58
9.1.2	Data analysis	60
9.1.3	Numerical analysis	61
9.2	Residential building in Vienna	62
9.2.1	Structure description.....	62
9.2.2	Field test	63
9.2.3	Data analysis and results	67
10	References	70
	Appendix: MoSeS: the AIT's MObile SEismic Simulator.....	72

List of Figures

Figure 1: Dynamic monitoring flowchart with links to closely related working tasks within NERA.	8
Figure 2: Steady state motion due to harmonic force.	11
Figure 3: Response factor for a one-story structure subjected to harmonic force.	11
Figure 4: Evaluation of damping from forced vibration tests.	13
Figure 5: Two-story building subjected to forced vibrations (a); free-body diagrams (b). ...	14
Figure 6: Response factors for a 3-story building subjected to harmonic force (Chopra, 2007).	16
Figure 7: Common signal types used for modal tests: (a) harmonic (sinusoidal), (b) periodic, (c) transient, and (d) random (Crocker, 2008).	18
Figure 8: Typical FRF measurement using sinusoidal excitation signal (Crocker, 2008).	18
Figure 9: Inertial shaker. (a) Mass exciter with two rotating masses of NEES@UCLA; (b) sketch showing the acting forces (nees@ucla).	20
Figure 10: Cross-section schema of electrodynamic shaker (Lang, Electrodynamic shaker fundamentals, 1997).	21
Figure 11: Impact hammer (Brüel & Kjaer).	22
Figure 12: General layout of a measurement system (Crocker, 2008).	26
Figure 13: Shaker attachment types: (a) rod attachment; (b) reaction mass exciting the foundation soil; (c) direct attachment	30
Figure 14: Connection of the shaker to the structure through a) a rod or a rod-chain ending with a plate (for RC structures or frame structures, b) a rod or rod-chain ending with a bar (for masonry structures), c) a hook for steel structures or bridges. d) Particular of the hook.	31
Figure 15: Position of the shaker connected to the structure with a rode.	31
Figure 16: Aliasing error due to insufficient sampling; (a) in the time domain; (b) in the frequency domain.	33
Figure 17: The Fourier transform of a continuous rectangle signal; (a) in the time domain, (b) in the frequency domain.	33
Figure 18: The discrete Fourier transform of a sampled rectangle signal at a sampling frequency of 5 Hz (a).	34
Figure 19: The discrete Fourier transform of a sampled rectangle signal at a sampling frequency of 10 Hz.	34
Figure 20: Leakage error due to non-periodicity when measuring a sinusoidal signal of 1 Hz; (a) sampling duration of 3s; (b) frequency content; (c) sampling duration of 3.5s; (d) frequency content.	35
Figure 21: The effect of measurement length on leakage error; (a) Measurement duration of 3.5s; (b) frequency content; (c) Measurement duration of 6.5s; (d) corresponding frequency content.	36
Figure 22: Basics of modal testing. (a) Modal parameters cannot be measured directly; (b) Modal parameters can be derived from the (linear time invariant) model of the identified structure.	37
Figure 23: Instrumentation layout of SFSI field tests performed at EuroProteas	44
Figure 24: H/V ratios for the instrument T5860 on the roof slab. The instrumentation layout of the roof slab of EuroProteas is also shown.	46

Figure 25: H/V ratios for the instrument T5861 at the corner of the roof slab. The instrumentation layout of the roof slab of EuroProteas is also shown.	46
Figure 26: Response at 3m distance from foundation (left) and at 9m from the foundation (right) (instrument 9084 did not perform in the NS direction).	47
Figure 27: Model configuration in MACEC.	48
Figure 28: Stabilization diagram of identified modes of EuroProteas.	49
Figure 29: (a) MK-500U schematic (b) Orientation of the mass plates [ANCO Engineers, Inc]	50
Figure 30: Output force against rotational speed of the shaker for different mass plates configurations.....	51
Figure 31: Recorded acceleration response at instrument T5856 for a series of tests according to the output frequency and the output force of the vibrator system.	52
Figure 32: Recorded acceleration in the soil in the vertical array for output frequency 8Hz and output force 17.51kN of the eccentric mass vibrator	54
Figure 33: Decay with distance of the recorded horizontal displacement from the vertical and horizontal SAARs for test #18 (output frequency 5.7Hz, output force 5.04kN)	55
Figure 34: Decay with distance of the recorded horizontal displacement from the vertical and horizontal SAARs for test #30 (output frequency 8Hz, output force 17.51kN)	55
Figure 35: The investigated building in Seibersdorf.....	58
Figure 36: Exciter position.....	59
Figure 37: Excitation using a rod chain.	59
Figure 38: Measurement layout: (a) 1st level (4.6m), (b) 2nd level (7.1m), (c) 3rd level (9.4m), (d) 4th level (9.6m), and (e) 5th level (12.0m).	60
Figure 39: Model grid.....	61
Figure 40: Calibrated FE-models (top left: 1st mode; top right: 2nd mode; bottom left: 3rd mode; bottom right: 4th mode)	62
Figure 41: Picture and drawings of the building.....	63
Figure 42: MoSeS parking	64
Figure 43: MoSeS' attachment to the building. (a) Rod chain positioning (b) Rod chain fastening to the building (c) Rod chain ready.	64
Figure 44: Sensors layout (a). Wired technology of sensors (b)	65
Figure 45: WN applied by MoSeS	67
Figure 46: Signal recorded in the measuring point 12y a) in the forced vibration test and b) in the ambient vibration test.....	68
Figure 47: Mode shapes identified from the ambient vibration testing data.....	69
Figure 48: Mode shapes identified from the forced vibration testing data.....	70
Figure 49: MoSeS' schema.	73
Figure 50: Electrohydraulic exciter and truck (a). Power unit (b). Pressure accumulator (c).74	
Figure 51: Diagrams of force-piston displacement for different frequency ranges and loads (0, 2 or 4 plates).....	75

List of the Tables

Table 1: 500U shaker eccentricity and maximum operating frequency 50

Table 2: Identified modes..... 61

Table 3: Comparison of model data and measurement values. 61

Table 4: Natural frequencies and damping ratios of the structure from the ambient vibration testing data..... 69

Table 5: Natural frequencies and damping ratios of the structure from the forced vibration testing data..... 69

2 Introduction

Knowledge about the dynamic properties of real structures is of increasing importance to the research and engineering community. The design of new structures and the assessment of existing structures to withstand seismic loads, strong winds, and many other types of dynamic forces require an understanding of the dynamic characteristics of each structure. To do so, the values of the natural frequencies, mode shapes, and damping parameters are required to be known. These values may be determined either by the elaboration of analytical models or experimentally through in-situ measurements. The experimental determination of the dynamic parameters is useful for the following reasons:

- to improve the state of the art by contributing to the general knowledge of the dynamic characteristics of structures,
- to determine the dynamic characteristics of structures which are difficult to model analytically,
- to validate the results of analytical models and eventually provide information for the adjustment of parameters of analytical models.

For these reasons the results of dynamic field test of existing structures contribute to improve both the design of new structures and the vulnerability assessment of existing ones.

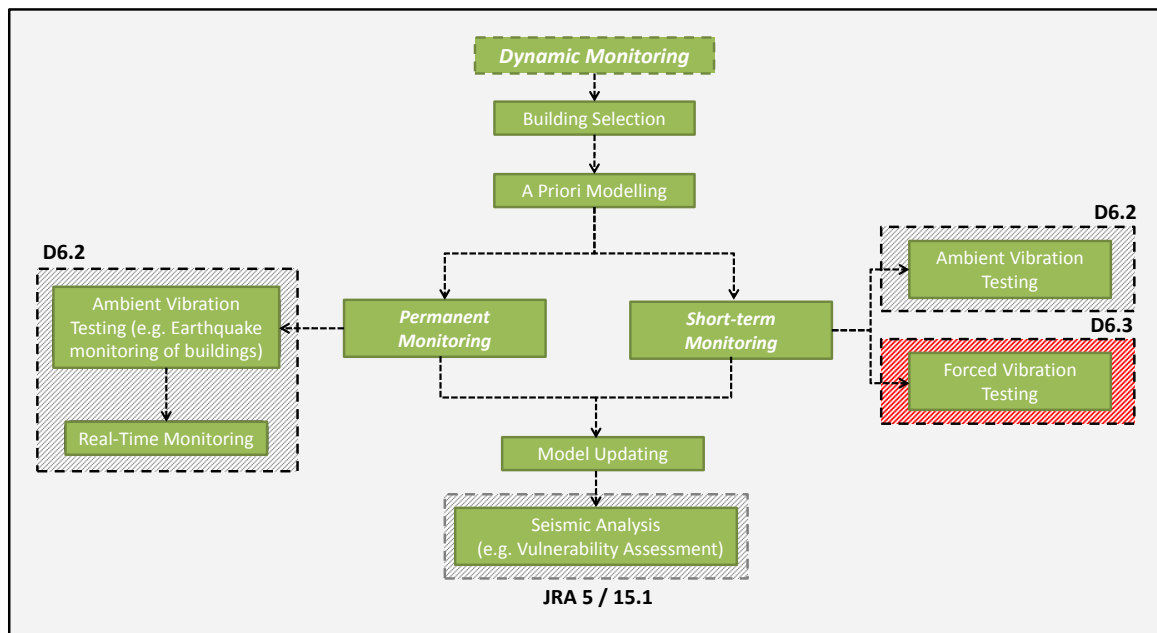


Figure 1: Dynamic monitoring flowchart with links to closely related working tasks within NERA.

2.1 Forced vs. ambient vibration testing

Dynamic field tests of structures are classified according to the nature of the excitation as either ambient vibrations or forced vibrations (Fig.1). In the *ambient vibration testing* the structural vibrations are caused by any kind of ambient sources like wind, traffic, walking people, eventual seismic events and other environmental or man-made loads. The ambient

excitations are characterized by random or pseudo-random or periodic signals. Forced vibrations encompass any motion in the structure induced artificially above the ambient level. Different force levels are available ranging from explosive devices to excite dam walls, large rotary eccentric mass shakers to excite horizontal motion in the upper levels of skyscrapers, to relatively small forces such as a person jumping. Each excitation method has its advantages and disadvantages and force/time characteristics that are suited to a particular structural excitation problem.

The ambient field testing is a popular method of gathering structural data as it is economical, non-destructive, fast, and easy to conduct.

However, certain drawbacks are associated with this method:

- lack of control over the timing, duration, amplitude and direction of the applied force,
- considerably lower signal to noise ratio than in the forced test mode thus making the post-processing much more challenging.

A further disadvantage of the ambient vibration testing is related to the identification process: most of the structural identification procedures based on ambient vibration data assume the excitation to be a white noise: this assumption is inaccurate in most of the cases and lead to imprecise or wrong system identification results.

Points in favour of *forced vibration tests*, on the other hand, are the favourable signal to noise ratio and the high controllability. The latter one includes the selection both of the desired frequency range, the intensity and direction of the exciting force amplitude and the duration of the excitation thus permitting a more targeted investigation of modal parameters. Although the forced vibration excitation can lead to assess detailed component behaviour, it is challenging due to practical difficulties associated with deploying a sufficiently large sensor array [Yu et al. 2004].

The downside of the forced vibration method is its inability to generate much force at low frequencies. In the case of eccentric mass excitation, for example, the amplitudes are proportional to the square of the excitation frequency, which limits its force in the low frequency range. On the other hand, the identification of the higher eigenfrequencies is easier from forced field testing data than from ambient testing data: this is a substantial advantage in model updating. Not surprisingly, as a vibration source is needed, this method also comes at a greater cost. Besides, it is more time consuming to conduct, need specific expertise and often require special permissions. Finally, the inability of artificial vibration sources to impart moderate-to-large amplitude vibrations on test structures and the inability of traditional vibration sources to excite structures with inputs that represent realistic simulations of broadband seismic excitation are limitation of the forced vibration method to not forget [Yu et al. 2004].

3 Mathematical treatise on forced excitation

3.1 Forced vibration applied to a single storey building

The expression “forced vibrations” indicates a vibrations produced by a force that continues to excite the system for a long time during its motion. The load applied by some devices, like shaker, used in forced vibration testing produces forced vibration of the structure, while other load sources, like impact hammers or masses used in the pulled and released methods, produce free vibrations of the structure. In this second case the force is impulsive and the structural response depends on the intensity of the load. Instead the forced vibrations depend not only on the force intensity but also on the characteristics of the load in frequency

domain. In order to simplify the understanding without recalling any specialized book on structural dynamics, the mathematical treatise of the forced vibration is presented hereafter.

Several real external forces or forces applied during field tests can be considered as a superposition of more harmonic signals, so the mathematical treatise of the dynamic behaviour of a system excited by a harmonic force is firstly proposed. The mathematical treatise is proposed firstly for a Single Degree of Freedom (SDoF) system.

A generic harmonic force applied to the system depends can be expressed as a sinusoidal function varying with time: $p(t) = p_0 \sin(\omega t)$. The amplitude, or maximum value, of the load is p_0 , its period is $T = 2\pi / \omega$, and the circular frequency is ω (Figure 2). The equation of motion

$$m\ddot{u} + c\dot{u} + ku = p_0 \sin \omega t \quad (1)$$

can be solved by standard procedures to obtain the response of the structure in two parts: free vibration response plus steady state response. The free vibration response of a damped structure decays, so only the steady state response is considered. Figure 2 shows the steady state motion of the system occurring with a time shift θ / ω (where θ is the phase angle). The expression of the system response respect to the steady state response is

$$\frac{u(t)}{u_{st}} = D \sin(\omega t - \theta) \quad (2)$$

in which

$$u_{st} = \frac{p_0}{k} \quad (3)$$

$$D = \frac{1}{\sqrt{(1 - \beta^2)^2 + (2\xi\beta)^2}} \quad (4)$$

$$\theta = \tan^{-1}\left(\frac{2\xi\beta}{1 - \beta^2}\right) \quad (5)$$

and β is the frequency ratio (ω / ω_0), i.e. ratio of the harmonic force and the natural frequency of the system.

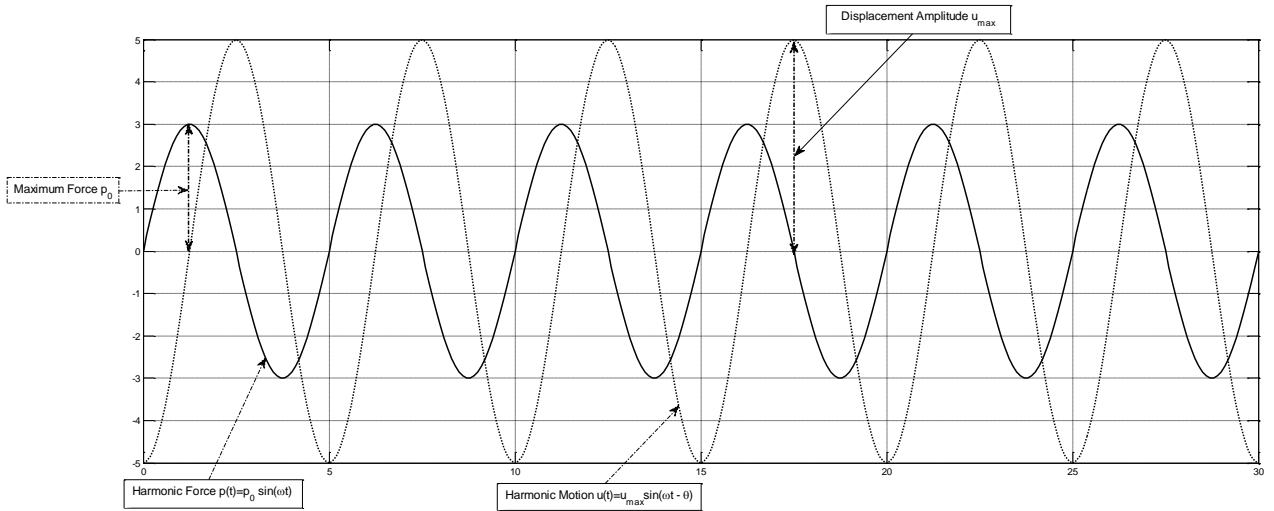


Figure 2: Steady state motion due to harmonic force.

The factor D is the ratio of the maximum amplitude of the dynamic displacement u_{\max} and the steady state response displacement u_{st} , i.e. the displacement that occurs when the force has constant intensity p_0 :

$$\frac{u_{\max}}{u_{st}} = D. \quad (6)$$

This factor D indicates the ratio of the maximum dynamic system displacement response to the static system displacement response. and depends on the parameters β and the damping ratio ξ , as the equation 4 shows. The Figure 3 shows this dependence: the values of D are calculated as function of β for several values of ξ .

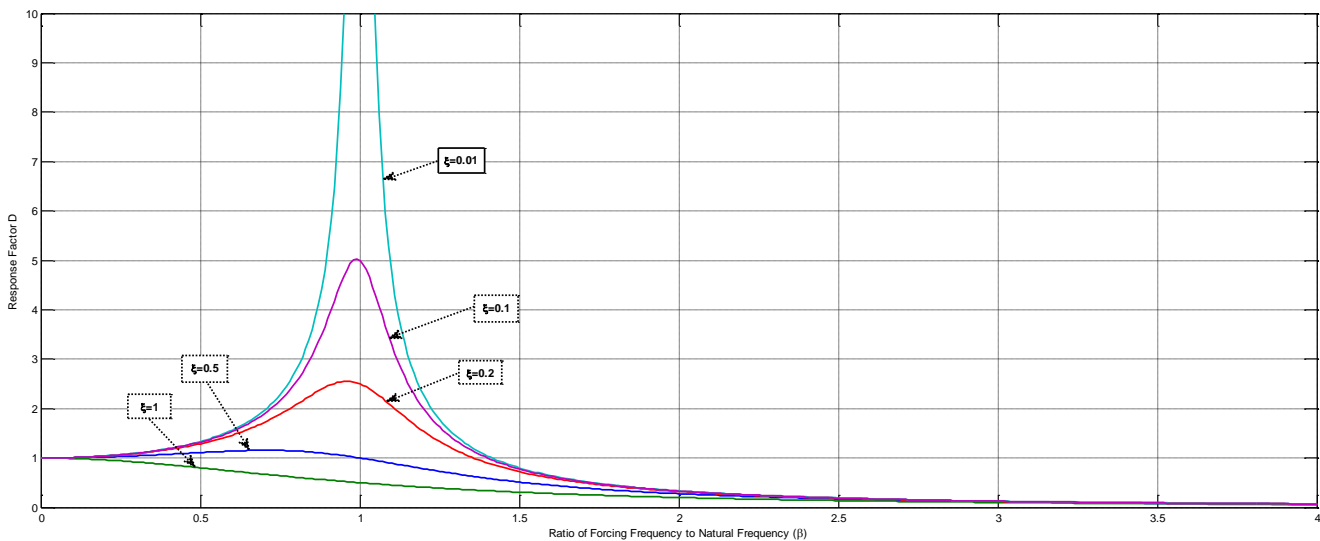


Figure 3: Response factor for a one-story structure subjected to harmonic force.

The Figure 3 leads to some observations.: For β close to zero, i.e. natural frequency of the external force extremely lower than the natural frequency of the system, the dynamic system response correspond to the static one ($D = 1$) for all the damping values of the system. For small values of β , i.e. lower frequency of the external force respect to the natural frequency of the system, the dynamic system response is higher than the static one. This means that the maximum displacement is controlled by the stiffness of the system with little effect of mass or damping. When $\beta = 1$, $D = 1/2\xi$, so the relation between the dynamic system response and the static one is inversely proportional to the damping ratio if the forcing frequency is the same as the natural frequency of the structure. For β close to 1, i.e. for resonance condition, the response factor is controlled by the damping ratio ξ with negligible influence of mass or stiffness. The maximum dynamic system response is obtained for this resonance condition. Finally, for value of β higher than one, i.e. frequency of the external force higher than the system natural frequency, the response factor is essentially independent of damping and approaches zero: the dynamic system response tends to be zero. It can be shown that at high forcing frequencies, the maximum displacement depends primarily on the mass.

For the resonance condition it is plain from the equation 4 that the peak value of D occurs at $\beta = \sqrt{1 - 2\xi^2}$. From this expression is possible calculate the displacement resonant frequency. Thus, the relations among the displacement resonant frequency, the damped natural frequency ω_D , and the undamped natural frequency ω are

- Displacement resonant frequency = $\omega\sqrt{1 - 2\xi^2}$,
- Damped natural frequency $\omega_D = \omega\sqrt{1 - \xi^2}$.

Although the displacement resonant frequency is different from the damped or undamped natural frequencies, the difference is negligible for the degree of damping typical of structures – less than 4% if the damping ratio does not exceed 20%.

For conditions next to the resonance one the damping of the system plays an important role to determinate the dynamic system displacement response. For values of $D = D_{\max} \div \sqrt{2}$, i.e. for 'half-power point', the width of β is 2ξ , as illustrated in Figure 4.

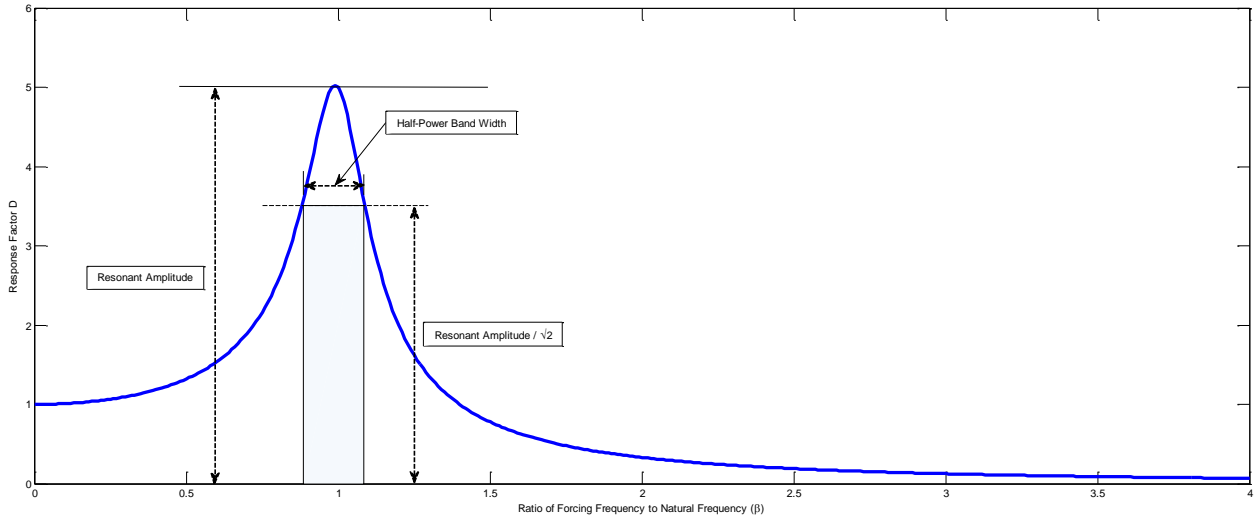


Figure 4: Evaluation of damping from forced vibration tests.

3.2 Forced vibrations applied to multistorey buildings

The equations of motion for a two-storey building (Figure 5.a) subjected to forced vibrations are hereafter presented. Subsequently, these will be generalized to obtain the motion equations in general form for a building with N storeys. The buildings are modelled as lumped mass system with the masses concentrated at the floor level (m_j).

External forces p_1 and p_2 applied to the floors of a two-storey building cause displacement of the floors themselves. For dynamic forces the floors displacement are variable with time ($u_1(t)$ and $u_2(t)$).

The forces acting on each floor mass m_j vary not only the external one forces $p_j(t)$, but also the ones produced by the interaction of that floor motion with the motion of the next floors, called elastic resisting forces f_{sj} , and the inertial one f_{Ij} , as the Figure 5.b.. The inertia forces act on opposite direction of the external force, while the elastic resisting forces act on opposite direction to the positive deformation. Each mass of the structure is in equilibrium at each instant under the action of these dynamic forces. For the two-storeys building the condition of dynamic equilibrium for the first floor mass is

$$f_{I1} + f_{s1} = p_1(t) \quad (9)$$

and the one for the second floor mass is

$$f_{I2} + f_{s2} = p_2(t) \quad (10)$$

The inertial and elastic resisting forces are related to the acceleration and displacements of the masses. For a linear structure, the elastic resisting forces are related to the floor displacements through the story stiffnesses k_j :

$$f_{S1} = f_{S1}^b + f_{S1}^a = k_1 u_1 + k_2 (u_1 - u_2) , \quad (11)$$

$$f_{S2} = k_2 (u_2 - u_1) ; \quad (12)$$

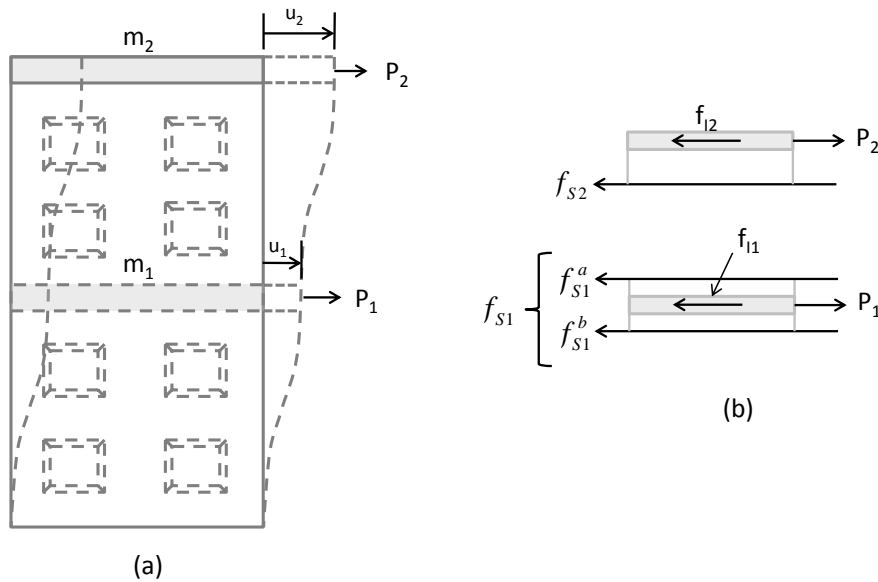


Figure 5: Two-story building subjected to forced vibrations (a); free-body diagrams (b).

Instead the inertial forces are associated with the masses m_j undergoing accelerations \ddot{u}_j :

$$f_{I1} = m_1 \ddot{u}_1 \quad (13)$$

$$f_{I2} = m_2 \ddot{u}_2 \quad (14)$$

Substituting the equations (11)-(14) into (9) and (10) the motion equations of the two floors are obtained:

$$m_1 \ddot{u}_1 + k_1 u_1 + k_2 (u_1 - u_2) = p_1(t) , \quad (15)$$

$$m_2 \ddot{u}_2 + k_2 (u_2 - u_1) = p_2(t) . \quad (16)$$

These two equations are not independent but coupled, therefore they must be solved simultaneously to determine the displacement response. Their solution can be calculated easily by means of the matrix form:

$$\begin{bmatrix} m_1 & 0 \\ 0 & m_2 \end{bmatrix} \begin{pmatrix} \ddot{u}_1 \\ \ddot{u}_2 \end{pmatrix} + \begin{bmatrix} (k_1 + k_2) & -k_2 \\ -k_2 & k_2 \end{bmatrix} \begin{pmatrix} u_1 \\ u_2 \end{pmatrix} = \begin{pmatrix} p_1(t) \\ p_2(t) \end{pmatrix} \quad (17)$$

For an N-storey building N motion equations must to be formulated and solved to calculate the dynamic response of the building to external forces.

3.3 Response to harmonic excitation

In case a multi-shakers field test is carried out and the dynamic forces applied to each floor are sinusoidal, the forces for the j-th floor appearing in the equation 17 become $p_j(t) = p_{0j} \sin \omega t$, where p_{0j} is the amplitude or maximum value of the force, $T = 2\pi/\omega$ is the period and ω is its circular frequency. The natural frequencies and vibrational modes of the building can be computed from the equation 17. For specific values of damping ratios ξ_n in the natural vibrational modes, the dynamic response of the structure to the harmonic forces can be determined by the mode superposition method.

As showed in the section 3.1 for one-storey building, the response of the structure consists of two parts: free vibration response plus steady state response. In a damped structure, the first part of the dynamic response decays so only the steady state response is considered. As shown in the equation 2, the frequency of the steady state response is the same as the external force, but the response is delayed with respect to the force due to the no-zero value of the phase between the force and the response.. Applying the equation 2 to the case of the N-storey building, the steady state displacement at the j-th floor can be expressed as

$$\frac{u_j(t)}{u_{j,st}} = D_j \sin(\omega t - \theta_j), \quad (19)$$

where $u_{j,st}$ is the displacement at the j-th floor of the structure if the maximum forces p_{0j} are applied as static forces and θ_j is the phase angle. Similarly to the equation 6 for the two-storey building, the amplitude of the dynamic response displacement at the j-th floor $u_{j,max}$ is

$$\frac{u_{j,max}}{u_{j,st}} = D_j. \quad (20)$$

The response factor D_j depends on the floor location, the forcing frequency, natural frequencies, vibrational modes and modal damping ratios of the building.

Figure 6 shows the case in which a harmonic sinusoidal external force is applied to the top of a three-storey structure with $\xi = 2\%$ for each vibrational mode. From the figure the resonance effect of each natural frequency of the building by means of the values of the response factor to each floor.

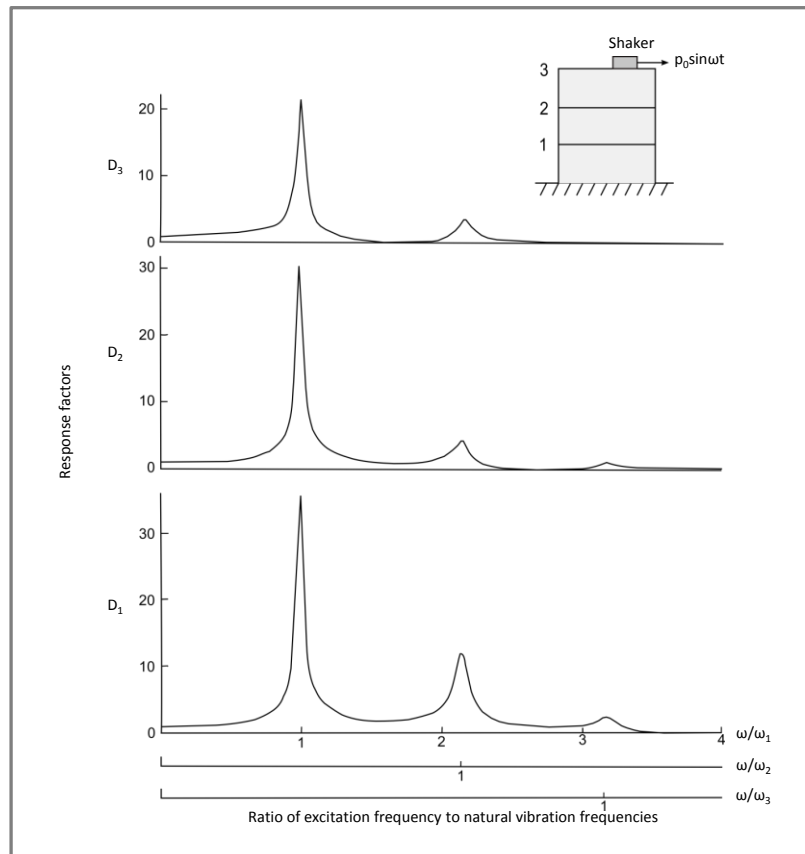


Figure 6: Response factors for a 3-story building subjected to harmonic force (Chopra, 2007).

While there are many factors to be considered in testing of complex structures, the basic approach outlined above leads to the calculation of the dynamic response of n-storey building to forced vibrations [(Chopra, 2007), (Clough & Penzien, 1995)].

3.4 Excitation Signals

The external forces applied in forced vibration field tests are nowadays synthetically generated like signals that drive the exciter. The signals describing the external forces can be classified in:

- Harmonic,
- Periodic,
- Random and

- Transient.

The class of the harmonic signals includes the signal characterized by a sine or cosine function. To generalize they are called hereafter sinusoidal signal. The dynamic external forces generated by the first shaker used in field testing of structures were sinusoidal. Nowadays this kind of external forces can be generated by all kinds of shaker. In field testing a sinusoidal force is applied to the structure for long enough time to excite the structure with a specific frequency and capture the structural response to that force, before exciting the structure with a sinusoidal force characterized by different frequency and measure the structural response to this different force. The natural frequencies of the structure have to be known before beginning the field test to select force frequencies close to them and obtain a condition close to the resonance one.

The force with a periodic signal can be generated only by complex shakers. The force signal is composed by a series of superimposed harmonic signals repeated with time period T . This kind of force excite simultaneously more vibrational modes of structure, so the field tests carried out applying it instead of the simple harmonic force are faster. The drawback of the application of this kind of force is relatively low signal strengths on each of its individual frequency components that often lead to average the structural response for a reasonable period of time in order to filter out background noise.

The random force signals are not deterministic, so they are generated always electronically and then reproduced by the shaker driven by a controller. Their generation is based on stochastic function. This force signal is the most complex force signal. On the other hand, the structural response to a force with random signal contains more information than the structural response to other kind of forces, but to extract it tricky methods have to be used. In order to obtain statistically reliable results both excitation and response signals have to be averaged for a considerable period of time. Despite the elaborate method used to analyse the forcing random signal and the structural response to it partial information affected by uncertainty can be extracted from them.

Different kind of force signals can be listed in the transient signal category. They are all characterized by a time variation. The impulse signal generated by the impact hammer is the most used transient load. Other transient signals are controlled sine pulse, single chirp and burst random signal. Free vibrations are the structural response to the impulse force, while a forced dynamic response is produced by continuous transient forces, like the single chirp or burst random one.

The methods used to analyse the structural response signal to random or continuous transient forcing signal use the spectral domain, so the analysis results are affected by uncertainty due to the Discrete Fourier Transformation (DTF). Figure 8 shows a typical frequency response function measured with a random excitation signal, including an indicator of quality (the coherence) on the response function.

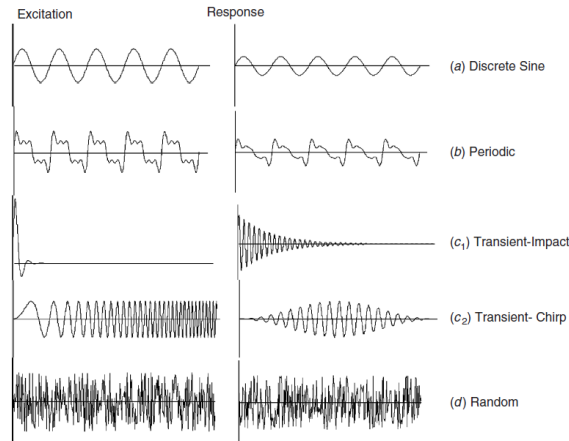


Figure 7: Common signal types used for modal tests: (a) harmonic (sinusoidal), (b) periodic, (c) transient, and (d) random (Crocker, 2008).

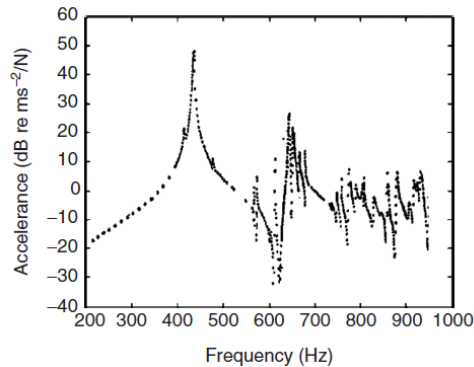


Figure 8: Typical FRF measurement using sinusoidal excitation signal (Crocker, 2008).

4 Methods of structural excitation

In this chapter the most common devices for vibration excitation of large-scale structures are presented, including their functionality, merits and disadvantages. The other methods used to excite the structure without any exciter are also shortly described.

4.1 Excitation devices

In full-scale testing of large-structures, exciters are generally of the contacting type, e.g. the exciter stays in contact with the test structure throughout the testing period. In such applications, they are physically mounted onto the structure. The contact exciting devices are called mechanical shakers and can be classified respect to source of vibration in:

- inertial shakers,
- hydraulic shakers and

- electromagnetic shakers (Harris & Piersol, 2002).

In case the structural free vibrations are the object of investigation an impulsive load is applied to the structure. This kind of load is produced by impact non-contacting devices. These impact device excite the structure during a short contact time and do not stay in contact with the structure during the record of the structural transient response. They are classified in:

- hammers and
- impactors.

The impulsive force applied to the structure with these devices is fully controlled and measured by a control sensor [(de Silva, 2005), (Brüel & Kjaer)]. In some special cases or for economic reasons other methods can be used to excite a structure with an impulsive load. The "pull-back and release" method is the most common and economic to apply an impulsive load to the test structure. In special application the blast of small explosive charges is used to excite the test structure with an impulse load.

The hammers and the pull-back and release method act in different way on the structures. The hammers produce an initial velocity of the structure, while the pull-back and release method produces an initial displacement of the structure. The hammers are used to test small parts of large structures, whereas the pull-back and release method is appropriate to the test a whole structure analysing its transient response.

4.1.1 Inertial shakers

An early form of exciter is the eccentric rotating mass shaker which is a reaction type mechanical vibration machine. It generates the vibratory force by using a rotating shaft carrying discs whose centre-of-mass is displaced from the centre-of-rotation of the shaft (de Silva, 2005). Often the discs are gears having slots where additional mass can be placed. The rotating shaft is driven by an electric motor (Harris & Piersol, 2002). The motion generating the force is circular while the force generated is monodirectional and sinusoidal. The magnitude of the applied force is constant for a particular setting of mass, rotational speed and the out of balance displacement. The rotational speed the shaft is selected as function of the frequency of structure to test and the mass added depends on the intensity of the exciting force to generate. Adequate shaft speed control is necessary in order to have satisfactory results. Inertial shakers with special configurations of the rotating discs can produce bidirectional forces or combination of sinusoidal forces. The dependence of the force intensity from the mass is the main disadvantage of this kind of shakers, due to the difficulty to move and place in heavy device.

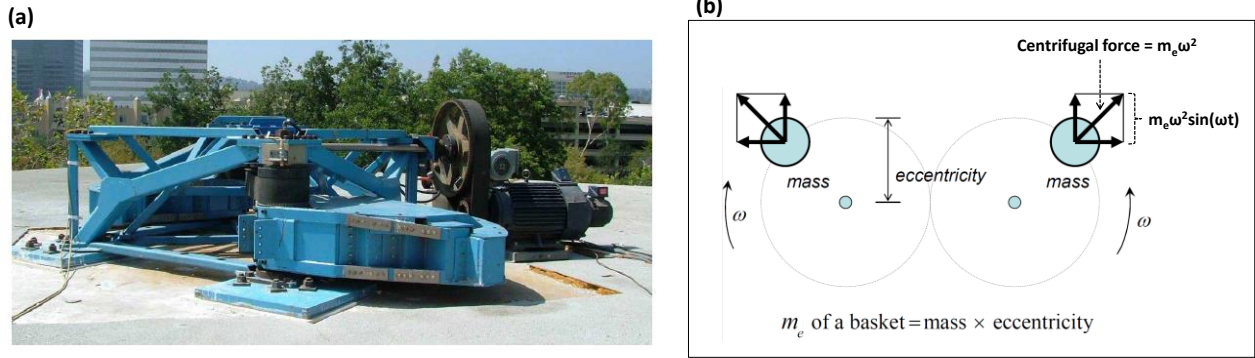


Figure 9: Inertial shaker. (a) Mass exciter with two rotating masses of NEES@UCLA; (b) sketch showing the acting forces (nees@ucla).

4.1.2 Electrohydraulic shakers

The electrohydraulic shakers are the most used shaker for field testing of civil structures due to their versatility. The force is generated through high-pressure flow of a fluid. The fluid is pumped into a cylinder with a piston by a pump. The pressured fluid pushes up the piston of the cylinder producing a force. The flow entering into and going out of the cylinder is regulated by a servo-valve. A control system checks the piston motion and drives the valve in order to get the exciting load defined during the first step of the field test. Additional mass is added to the piston to change the intensity of the generated exciting load. The weight of the mass can be varied to obtain varying force magnitudes. The pump is driven by an electric motor [(de Silva, 2005), (Harris & Piersol, 2002), (Stokoe, Menq, Wood, Rosenblad, Park, & Cox, 2008), (Cuhna & Caetano, 2006)].

This kind of shaker generates sinusoidal, static or random load. The vibrators provide relatively high vibration strokes and allow accurate excitation at different frequencies in bending or torsion. They also have the advantage of being able to apply static preload and complex waveforms to the test structure. However, the downside is their inability to excite in the higher kHz range – only very specialized exciters can operate in the range above 1 kHz, but the characteristic frequencies of civil structures are lower than this value.

4.1.3 Electromagnetic shakers

Electromagnetic shakers are often named electrodynamic exciters. The structure of an electrodynamic shaker somewhat resembles a common loudspeaker. At the heart of the shaker is a coil of wire, suspended in a fixed radial magnetic field. When a current is passed through this coil, an axial force is produced in proportion to the current and this is transmitted to a piston. The magnetic field in which the wire coil is suspended is created magnetizing permeable steel or iron elements by means of a permanent or an electromagnet. The magnet is placed inside a cylindrical and hollow element made of magnetic permeable iron or steel. This cylindrical element is closed at the base with a disk of the same magnetic permeable material. The south pole of the magnet is placed in the middle of this disk. Another cylindrical element of magnet permeable material is placed on the north pole of the magnet up to the upper end of the external hollow cylinder. The magnet flux is

conducted through the elements of magnet permeable iron and steel: the inner cylinder becomes the inner or negative pole of exciter and the external hollow cylinder is the outer or positive pole. Due to the shape of the two poles a radial electromagnetic field is generated. The air gap between the two poles of the system has to be reduced to maximize the intensity of the magnetic field.

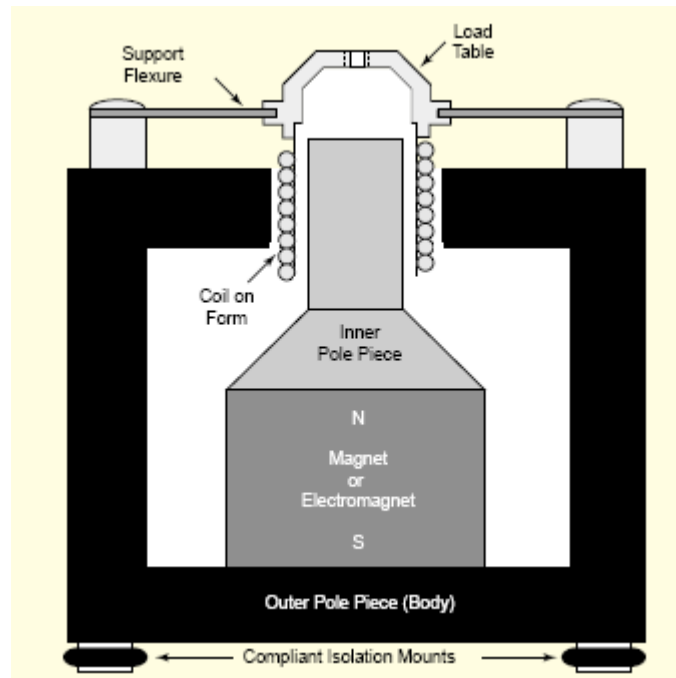


Figure 10: Cross-section schema of electrodynamic shaker (Lang, Electrodynamic shaker fundamentals, 1997).

The monodirectional force provided by the machine is proportional to the magnetic flux passing through the coil, to the current flowing through the coil and to the length of wire coil within the flux field, which is normally longer than the positive pole. In more complex electrodynamic shaker the magnetic field is generated by stationary electromagnets. These electromagnets are made by wire coiled up round ferromagnetic elements and the magnetic field is generated when the electric current flows through the wires. The dynamic element is also a wire coil which a piston is mounted on [(de Silva, 2005), (Lang, Electrodynamic shaker fundamentals, 1997) (Lang & Snyder, Understanding the physics of electrodynamic shaker performance, 2008), (Harris & Piersol, 2002)].

In the past, electrodynamic shakers were frequently used to drive shaking tables. Today smaller shakers are used in lab and field. For field tests, strong electrodynamic shakers are not useful because their cost is considerably greater than the cost of electrohydraulic shaker. Therefore mainly small electrodynamic shakers are used for in-situ investigations to excite structural members such as slabs or walls.

4.1.4 Impact hammers

The impact hammers are used in civil structures to test small parts of them. These devices are used to strike the part to test of the structure exciting it with an impulsive force. The hammer has a piezoelectric or strain-gauge type force sensor at its tip to measure the force applied during the impact. This sensor is called load cell and produce a signal proportional to the force applied and sent it to the input. In some sophisticated device the tip sensor measures not only the force but also the acceleration. The hammer can be provided with different tips characterized by specific hardness to concentrate the produced excitation in a narrow range of vibrations (nees@ucla).

The experience of the operator in the hammer impact test is extremely important, because the firmness in holding the device, the velocity and unicity of the impact influence the test results.



Figure 11: Impact hammer (Brüel & Kjaer).

4.1.5 Pull and release methods

Some impact dynamic tests can be carried out pulling an object fixed to a floor of the structure and releasing it. The mass of the object to pull and release has to be high enough to excite the part of the structure to be tested. The force applied to the structure depends also on distance of release. The material which the pulled and released object is made of influences the results of the test to avoid multiple impacts. The mass of the object to release has to be harmonized with its shape and the resistance of the wall or floor which it has to impact on.

This kind of force vibration method is carried out releasing an object to the floor. In that case the characteristics of the floor influence the results of the tests.

This kind of test is extremely cheap and do not require additional instruments respect to the ambient vibration tests. The drawbacks are hard controllability of the test and the quality of the test results. Moreover, the dynamic test carried out pulling and releasing an object is useful to test small parts of the structure.

Some attempts to use this method to excite a whole building have been made. The object pulled and released is in that case the structure itself. A group of people pull a rope firmly attached to the structure. When a small displacement of the structure occurs, the people release the rope and the free vibration response of the structure can be recorded.

4.1.6 Other excitation mechanisms

For multi-storeys building and bridges the natural frequencies a-priori estimated can be validated exciting the structure at these frequencies through a group of people jumping. This method is frequently used due to its low cost. In case of structures it can be applied only in buildings with stiff diaphragms.

Most of the electrohydraulic and electrodynamic shakers can be used also as mass reactors. This operational mode is used to test the soil or some structures, like bridges and dams. A single impulsive force or a series of forces can be applied to the soil or structure and the free vibration response or the forced vibrations response followed by the free vibrations ones can be recorded and analysed.

5 Methodology

5.1 Test planning

The basic concept of a forced vibration test is to measure the vibration response to a controlled and known force (the force in the pull and release method or in the excitation applied with a group of people jumping is not really controlled or known). One of the primary issues in the planning phase concerns the selection of a suitable exciter – depending on the objectives of the measurement campaign and the size of the test structures, one can choose from a range of exciters. Special consideration must be also given to the excitation signal itself which can generally be sinusoidal, periodic, transient or random (see §2.4). Another decision to be made is where the excitation should be applied for maximum effect. Here, it is important to determine the excitation spot according to the desired vibration modes (Ewins and Crocker 2007).

Likewise, for the response transducers, it is recommended to carefully choose the ones with a suitable sensitivity to the vibrational characteristics of the structure to test. The layout of the sensors is also extremely important for the correct interpretation of the measures. Failure to measure at sufficient points will make the results difficult to interpret. The measurement points should be thick enough to make the distinction between two modes of similar shape possible.

In order to plan a successful forced vibration test of a structure a preliminary study of the drawings, inspections of the structures and static and dynamic analysis of a preliminary model of the structure are advised.

In the planning process of forced vibration tests the following phases are picked out:

- Classification of the structure to test (kind, material, primary elements),
- Identification of the structural characteristics to value,
- Selection of the forced vibration testing method to apply,
- Calculation of the force to apply and duration of the excitation for continuous force methods,
- Design of exciter attachment to the structure if a shaker is used,
- Design of the sensors grid and selection of the technologies for the data acquisition.

The following sections explain some issues, with which to deal in the test planning.

5.2 Instrumentation

Final aim of the field testing is the collection of the data required for the dynamic identification process. The basic test setup required for making field tests depends on a few major factors. These include the type of structure to be tested and the level of results desired. Other factors, including the support fixture and the excitation mechanism, also affect the amount of hardware needed to perform the test. Despite the instrumentation and the acquisition system, some of the information describing every physical phenomenon will get lost, *e.g.* some of the high-frequencies harmonic components cannot be identified depending on the sampling frequency. Therefore, while choosing the instrumentation, the acquisition system and its set-up, it will be of primary importance to check whether or not the loss of information could lead to a significant loss of reliability of the results. This will clearly depend both on the acquisition system and on the desired level of accuracy characterising the identified quantities of interest.

In the paragraphs 4.3, 4.4 and 4.5, brief descriptions will be reported giving an overview about a standard acquisition system, the possible instruments to be used for dynamic field testing together with some indication about their positioning and their mounting on the investigated structure. It has then to be considered that a number of books and guidelines and national norms have been published in the past years on these arguments and they should be consulted for a complete description of these issues. The sections include also the description of instrumentation necessary to drive the shaker in forced vibration tests. For the choice of the forcing load to excite the structure is discussed in a different section.

5.3 Data acquisition board

The data acquisition system is the equipment required for the detection of the vibrations, their measure and the conversion and storing of data. The acquisition system, either analog or digital, generally includes these three following main hardware components:

- sensors;
- signal conditioners (data acquisition boards);
- recording system.

In case of forced vibration method the data acquisition system includes also signal conditioners to generate the signal driving the shakers and record the signal coming from the sensors on the shaker.

Different types of sensors can be used to detect the structural vibrations, as it will be discussed in the following paragraph. Despite the type of physical quantity (*e.g.* acceleration, velocity or displacements) measured by the sensors, signal conditioning may be necessary. Signal amplification and low-pass filtering with anti-aliasing function are two of the most common conditioning processes applied to the data. These functions are normally performed by the data acquisition boards that are also used to digitalise the signals coming from analog transducers.

More in detail, the acquisition board is a system performing all the operations required for data format conversion to allow interfacing the sensors and the data-storing system. As already mentioned, a signal conditioning method is generally applied to the input channels including amplification or attenuation, filtering and current-to-voltage conversion. Every input channel is then connected to a sample and hold (S/H) circuit: an analog device that samples the voltage of a continuously varying analog signal and holds its value at a constant level for a specified minimal period of time. Scope of this component is to eliminate variations in the input signal that could corrupt the analog-to-digital (A/D) conversion process. It is worth mentioning that the acquisition boards used for structural dynamic identification need to perform simultaneous sampling on all the connected instruments since the relative phase of the signals is essential information.

Besides the simultaneous sampling, the data acquisition boards have at least other two critical characteristics: the maximum sampling rate and the resolution of the analog-to-digital converter (ADC). The sampling rate of the acquisition system is function of three contributes: (i) the settling time required for the stabilisation of the input signal; (ii) the conversion time required by the ADC; (iii) the time required for transferring the sample to the buffer of the storage device. It is essential that the maximum achievable sampling rate is higher than the minimum required value that, in turn, depends on a number of parameters, such as the maximum structural frequency of interest (hence the Nyquist frequency) and the number of channels processed by the acquisition boards. Obviously, given the maximum number of samples per second that an acquisition board can process, increasing the number of connected channels will decrease the maximum achievable sampling rate.

Another important parameter is the sampling resolution of the ADC: while converting the analog signal coming from the sensors to a digital one ready for the storage unit, higher resolution will lead to a more accurate sampling. For most of the cases, a 16 bit resolution will be adequate; acquisition boards with higher resolution are available on the market, but their cost cannot always be justified since the electrical noise will cancel the benefit of the ADC resolution increase.

On the side of the recording unit, things are less complicate, since most of the commercial personal computers have performances compatible with the requirements of a standard acquisition system. Normally, the speed of a standard hardware is enough to write the data coming from the ADC to the storage unit. For some cases, when a very high sampling rate on a large number of instruments must be adopted, it is possible to use high-speed hardware (mother-boards and hard-disks) or particular hardware configurations. One of these is the Redundant Array of Independent Disks - RAID 0 - which allows an automatic subdivision of the data between two or more disks, clearly having great advantages both for the writing and the reading speed. Nevertheless, it is important to note that this solution is quite risky, since if one of the disks fails, the all array will fail too causing the loss of the recorded data.

Finally, additional components of most of the acquisition system are the cables used for connecting the different parts of the system itself. Although in the last years wireless technology is rapidly improving, the majority of the systems used for dynamic identification are still wired. When using cables for the connections, particularly between the instruments and the acquisition boards, their performances must be checked as accurately as those of the other components. In particular, the size and the length of the connection cables should not cause significant potential drop to the electrical feeding and output of the instruments. Furthermore, the cables should be adequately shielded to avoid external interference/noise on the recorded signals: particularly when working close to electromagnetic field sources, this can be of particular importance. From this point of view, examples of possible sources of

disturbance are elevators engines or other electric engines inside buildings, or the railway electric lines. Another possible source of disturbance is the cross-talk: this effect, negligible for most of the cases, can disturb the recording at very high sampling frequencies (about 10-20 kilo-sample per second) particularly when the connection cables are left in coils [(Harris & Piersol, 2002), (de Silva, 2005), (wilcoxon), (Brüel & Kjaer)].

5.4 Data acquisition boards for forced vibration methods

The forced vibrations exciting the structures can be produced by either forcing action not measurable or a shaker. In the second case the data acquisition boards has component to drive the shaker and record the signal coming for the sensors connected to the shaker. The data acquisition board has not only the input channels to receive the signal from the sensors, but also a double output and input channel for the shaker. In case the exciter mechanism is a basic instrumented hammer, only the input channel for the exciting device is used: the force applied and measured on board of the hammer is transmitted to the data acquisition board. To use a shaker the data acquisition board generates the signal and converts it from digital to analog through a Digital-to-Analog Converter. The analog signal is amplified by a power amplifier and sent to the shaker. The force applied from the shaker is measured by a sensor, on board either of the shaker or of the connection of the shaker to the structure. That sensor is called control sensor (Harris & Piersol, 2002). In case the force measured form control sensor is different from the one estimated generated by the data acquisition board a controller modify a signal sent to the power amplifier.

The power supply for signal conditioning may be voltage or charge mode and is sometimes provided as a component of the data acquisition board.

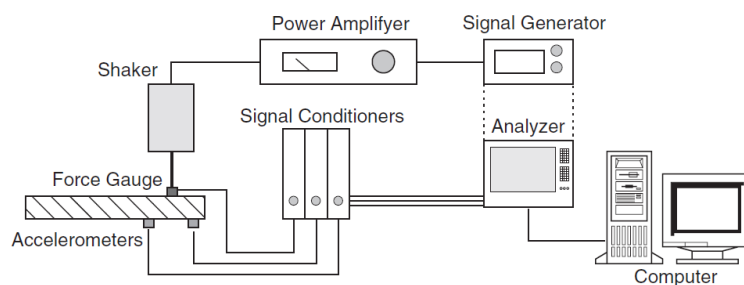


Figure 12: General layout of a measurement system (Crocker, 2008).

5.5 Types of sensors

The methods for measurement of vibration may be different in relation to characteristics of the excitation and in particular to its intensity, the response of the structure under investigation and the aim of the study undertaken. Therefore, the choice of the type of transducer must be made taking into account a series of parameters, such as the vibration amplitude and the frequency range of interest.

The motion can be measured by any of the kinematic quantities characterizing it, *i.e.* acceleration, velocity and displacement. However, it is worth to mention that:

- the acceleration is the easiest quantity to be measured thanks to the availability of instruments (accelerometers) with different characteristics, *e.g.* sensitivity, frequency response and robustness;
- the velocity is often used as response quantity, nevertheless the existing instrumentation, although very efficient and reliable, it is limited in the response at low frequencies. For this reason, especially when the structural response has significant component at low frequency, it is preferable to record acceleration. Then, if the adopted analysis method requires velocity measures, it is common practice to obtain them by integration of the signal. This operation, however, can introduce errors despite the adoption of analog or digital integration procedures;
- the absolute movement is probably the most difficult quantity to measure, nevertheless advantages can derive by the fact that no-contact instruments (interferometer) can be used.

When the choice is to measure the acceleration response, accelerometers and servo-accelerometers should be used, because they are more widespread than the one measuring the velocity. The sensors measuring the acceleration have an inner mass, the dimension of which depends on the operative frequency range that vibrates generating the signal. Different physical principles can be used to produce the signal, mainly two accelerometer types can be used: piezoelectric and capacitive. The first type is preferable for measuring high frequencies, while the latter generally has its best response in the medium frequency range. Servo-accelerometers are almost the same as accelerometers, but they include a system for signal amplification. This kind of transducers can be used to overcome the problem, characterising the accelerometers response, of having signal amplitude proportional to the displacement, hence low signal for small induced displacement. Nevertheless, when using forced vibrations to characterise a structure, accelerometers can be used quite effectively.

Seismometers, or geophones, can be used to measure velocity. These instruments contain an internal mass that can move relatively to the instrument frame. Mass and frame are connected by a flexible system (such as a spring) that holds the mass fixed to the frame if there is no motion, and damps out any movement if the external frame stops. Furthermore, a means of recording the relative motion of the mass to the frame, or the force needed to keep it from moving, is included in the instrument. Any motion of the structure to which the instrument is connected moves the frame, while the mass tends not to move because of its inertia. The relative velocity between frame and mass is therefore a measure of the structural movement. The geophones used for structural applications are generally very sensitive; hence they can be successfully used for detection of small ambient vibrations. Strong movements, as those caused by forced vibrations, can easily go out-of-scale.

Laser or radar interferometers are used to detect structural displacements. Although based on different physical principles, both instruments have an emitter, respectively producing a laser beam or electromagnetic waves, and a receiver, detecting them after the reflection against the structure under investigation. The distance between the instrument and the structure is evaluated at very high rate leading to the determination of the structural movements (*i.e.* variation of distance). These instruments have some big advantages that sometimes represent their limitations too:

- the measurement is performed with no-contact to the structure, that on the other side means that an adequate open space must be available in order to place the instrument and frame the structure;
- these instruments can detect displacements of a few microns from 200 m in the frequency range 0.1 - 150 Hz, but vibrations of the instruments can strongly affect the results as the actual measured quantity is the relative distance between the instrument and the structure.

For operation the wired sensors require a power supply. Some sensors have internal circuitry that allows the data acquisition board to provide the power, eliminating the need for a power supply. It includes a calibration setting that allows the voltage signal to be converted back into a measurement of acceleration/velocity. The wireless sensors include also an independent power supply.

Manufacturers calibrate each sensor and give it a sensitivity value. Accurate measurements depend mainly on using a sensor with the right sensitivity for the application. On the other hand the correct sensitivity value has to be used to process the data collected. If high values of the physical quantity measured by the sensors are expected, a too high sensitivity could lead to a saturation of the input circuitry on the signal analyser. If the signal level is very low, a small sensitivity may produce a signal that is too weak to accurately measure. Sensitivity also has an important impact on the signal to noise ratio. Signal to noise is the ratio of the signal level divided by the noise floor level and is measured in the dB scale as

$$S/N = 20\log\left(\frac{Signal}{Noise}\right) \quad (22)$$

All sensors and measurement hardware are subject to electronic noise. Even if you know that the sensor is not moving, electronic noise may induce some small signals. This is due to the sensor cables picking up electronic noise from stray signals in the air, from noise in the power supply or from internal noise in the analyser electronics. High quality hardware is designed to minimize the internal noise making low signal measurements possible. The signal to noise ratio limits the lowest measurement that can be made.

In general, it is a good practice to not trust a measurement with a signal to noise ratio that is below 3:1 or 4:1. When the signal to noise ratio is too small, one solution is to use a sensor with a higher sensitivity. Some sensor power supplies include a gain setting that multiplies the signal by 1, 10, or 100. Unfortunately, this setting also multiplies the noise that is picked up by the wires and inherent in the sensor and power supply. In most cases, increasing the power supply gain will not solve signal to noise problems [(Dorf, 2000), (de Silva, 2005), (Harris & Piersol, 2002), (LDS DACTRON)].

5.6 Attachment to the structure

The attachment of the exciter to the structure is a critical point in forced field tests carried out with shakers. The connection depends on the shaker and the part of the structure to excite. For small shakers used to excite a part of the structure, like a floor of a building, it is necessary to connect the driving platform of the shaker to the structure (see Figure 13.c). It is important to check the correct placement of the shaker on surface that as to not be covered with material smoothing out the force applied by the shaker.

When a large power shaker is used to excite the whole structure, the attachment to the structure depends on several factors:

- the force to be applied to the structure,
- the kind of shaker and its versatility,
- the accessibility of the structures and the location of the structures and
- the kind of structure and its height.

Inertial shakers often cannot be plugged to the structure, but they just perform the excitation through the foundation soil, as illustrated in Figure 13.b. In some special cases these shakers excite the structure being connected to a wall of the ground floor of the structure, as in Figure 13.a. This excitation modality is possible only with inertial shakers that can operate in horizontal direction and on special reinforced industrial structures.

Electromagnetic and electrohydraulic shakers have often more operation modalities: they can perform the excitation working as shaker connected to the structure through a chain or bar or working as reaction mass. The force transferred by the shaker to structure depends on the operational mode. The operational mode is related to the kind of structure to test and its accessibility. Most of the masonry structures, like the one tested in the second case study described in the last part of these guidelines, or frame structures cannot be excited by a shaker operating like a reaction mass in horizontal direction. In case of structures in a built-up area the shaker working as reaction mass in vertical direction bothers the population of a large area: for that reason this operational mode is used mainly to test infrastructures, like small massive road bridges or obviously the foundation soil.

The accessibility of the structure to test is extremely important to define the connection of the shaker to the structure. The accessibility depends mainly on the shaker transportability. Most of the forced field tests on low or middle height structures are carried out with electrohydraulic and electrodynamic shakers, not operating as reaction mass. The shaker is plugged to the structures by a rod or a rod-chain, as aforesaid (Figure 13). The rod is fastened to structure by a bolted plate in case of a reinforced concrete structure (Figure 14.a), by a bar going across a window (Figure 14.b) or a rod going across a window and wrapping a whole interior wall up in case of masonry structure and by a hook in case of steel structure (Figure 14.c and 14.d).

Depending on the shaker mass and the accessibility of the desired excitation location, one option is to directly plug the device to the structure. Sometimes, however, it is simply not feasible to transport the shaker to a location within the building and the structural excitation has to be performed from outside the building with a rod, as illustrated in Figure 13.a.

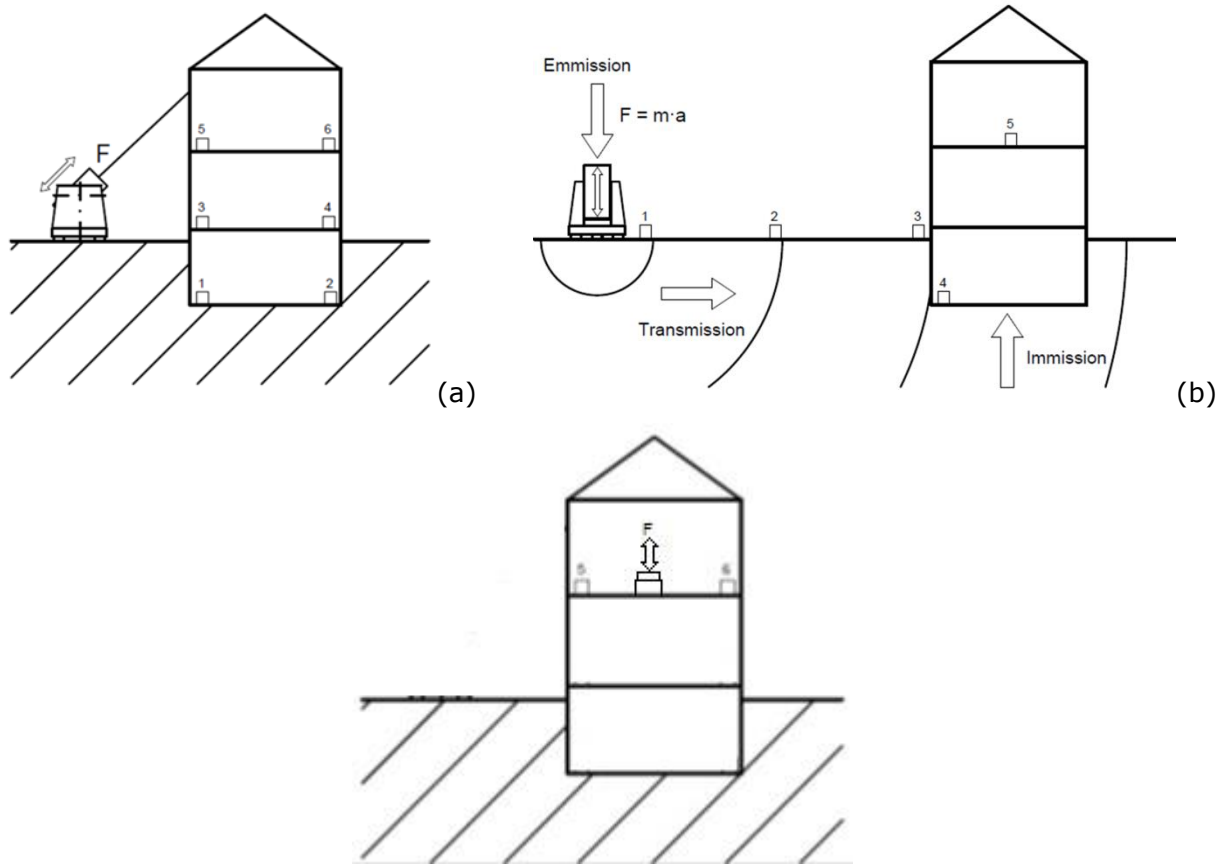


Figure 13: Shaker attachment types: (a) rod attachment; (b) reaction mass exciting the foundation soil; (c) direct attachment



(a)



(b)



(c)



Figure 14: Connection of the shaker to the structure through a) a rod or a rod-chain ending with a plate (for RC structures or frame structures), b) a rod or rod-chain ending with a bar (for masonry structures), c) a hook for steel structures or bridges. d) Particular of the hook.

5.7 Positioning of the exciter

The exciter has to be positioned on the structure or connected to it in a way to excite both the symmetrical and asymmetrical modes, when the structure is symmetric. In case of asymmetrical structures the exciter has to apply the force in a way to get the maximum motion for each mode to investigate.

Excitation force produced by the shakers is monodirectional, so the shaker has to be positioned respect to structure in order to excite it in more than one direction. In case the load excitation is applied to the structure through a rod or a rod-chain the shaker has to be located to excite the structure in both the two main horizontal directions. The height to which the shaker is attached by means of a rod or rod-chain has to be the highest of the possible ones to amplify the shaker excitation. Some general indications are given in the Figure 15. In case the structure has share walls the position of the exciter is affected by them.

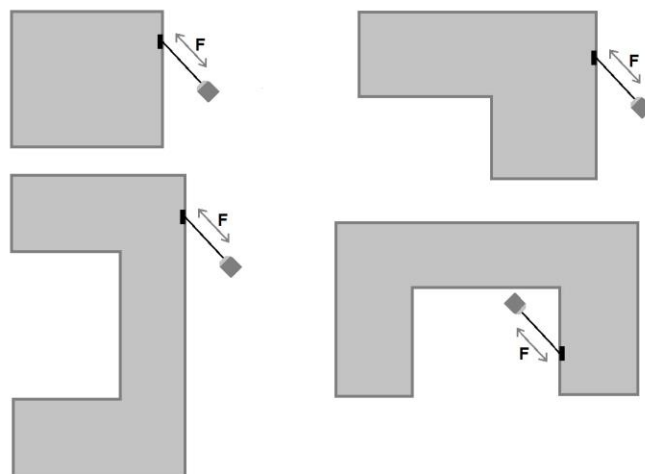


Figure 15: Position of the shaker connected to the structure with a rode.

5.8 Shaker selection

The choice of the shaker to be used in forced field testing is function of many factors:

- the kind of exciting signal that it can produce and
- the maximum power of the shaker.

The issue of the different exciting signal is approached in the previous section. The other factors to take into account in the shaker selection are here analysed. The performance curve describes in effective way the shaker characteristics: the peak velocity the shaker can produce on the structure is related to the range of operating frequency of the shaker. The maximum displacement imposed by the shaker to structure is constant to the low frequencies, while the acceleration impressed by the shaker to structure is constant at the high frequencies of its operating frequency range. The middle frequencies of this range are dominated by constant velocity produced by the exciting device on the structure. The maximum acceleration that a shaker can produce on the structure depends on the mass of the structure; therefore for increasing value of the mass, the operating frequency range of the shaker has smaller amplitude.

The shaker mass and the acceleration of the shaker are proportional to the maximum force that a shaker can produce. The real force applied to structure can be different from the maximum force produced by the shaker and their ratio depends on the kind of connection of the shaker with the structure: this force ratio has unit value only in case of rigid connection.

6 Data processing and interpretation

6.1 Quality control and data filtering

The objective of a vibration field measurement is to acquire sufficient information (data) in order to apply selected methods of system identification with a certain degree of confidence. The measurement length or precisely the data set length used in system identification must be adequate to be considered as periodic in time. This requirement is dependent on:

- (i) The level of noise presented;
- (ii) The nature of the excitation sources;
- (iii) the damping characteristics and;
- (iv) The complexity of the structure.

During vibration based field measurement, the continuous structural responses are sampled to discrete time histories. This digitization process may lead to errors. The most common one is aliasing error, which originates from high frequency components causing amplitude and frequency errors in the spectrum. To avoid this error, all frequencies higher than half of the sampling frequency should be removed with a built-in low-pass filter of the data acquisition system. From a practical point of view, the sampling frequency has to be at least more than twice the highest frequency of interest. The frequency range of interest depends upon the distribution of spectral content over the frequency range of the excitation and upon the structural response of the structure. This recognizes the spectral content as the most important property of vibration input.

Figure 16 shows an example of the aliasing error due to insufficient sampling. The harmonic signal with a frequency of 1 Hz is sampled at a sampling frequency of 0.9 Hz. This low sampling frequency causes an alias signal of 0.1 Hz.

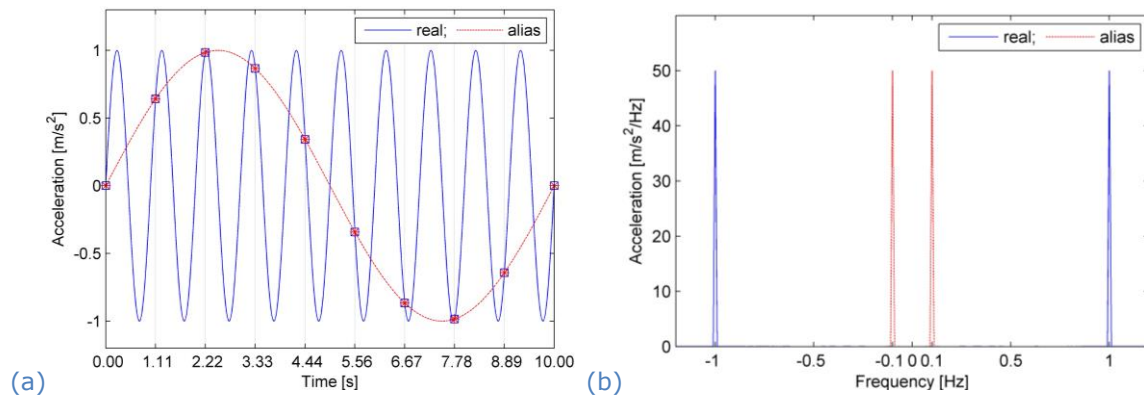


Figure 16: Aliasing error due to insufficient sampling; (a) in the time domain; (b) in the frequency domain.

If there are slow drifts in the data that suggests low frequency disturbance (blurring) or noise, a high-pass filter might be applied with suitable cutoff frequency in order to remove that unwanted signal component. Zero-phase digital filtering of the acquired data can also be employed in both forward and reverse directions. Finally, we might need to down-sample the data to the frequency range of interest to reduce the computational cost of system identification due to over-sampling.

The following discussion will make known other errors, mainly caused by the digital sampling process and as a result of assumption violation during a discrete Fourier transform. Figure 17 is a continuous rectangle signal and its continuous Fourier transform.

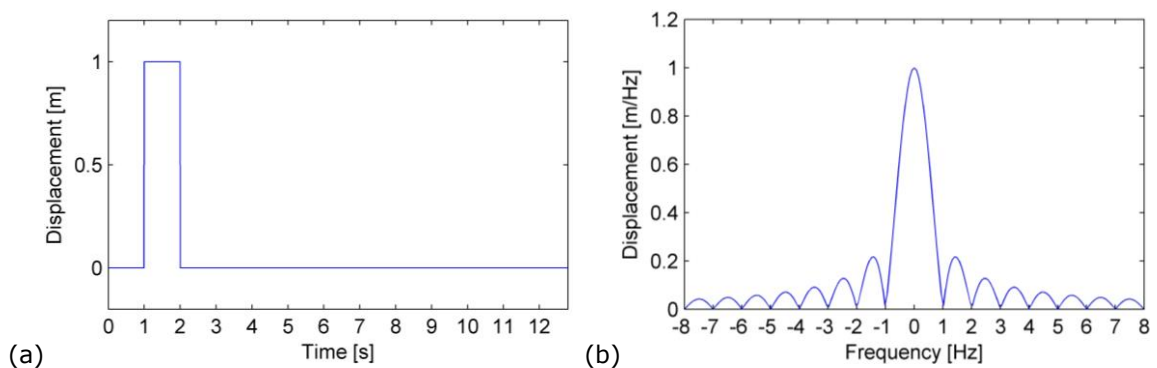


Figure 17: The Fourier transform of a continuous rectangle signal; (a) in the time domain, (b) in the frequency domain.

In the measurement process, this continuous signal has to be sampled by digitization, supposed to be at 5 Hz in this example. The low sampling frequency setting causes erroneous results in the frequency domain (see Figure 18). However, by doubling the

sampling frequency to 10 Hz, the discrete Fourier transform results have already approached the continuous one as in Figure 19.

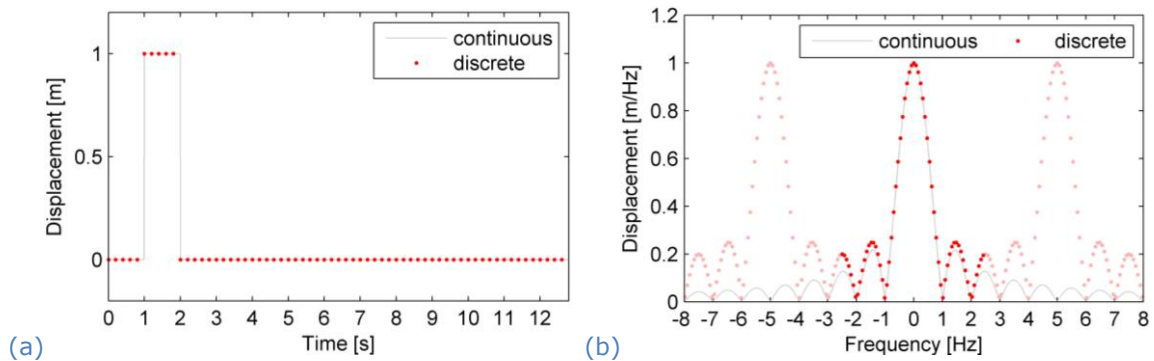


Figure 18: The discrete Fourier transform of a sampled rectangle signal at a sampling frequency of 5 Hz (a).

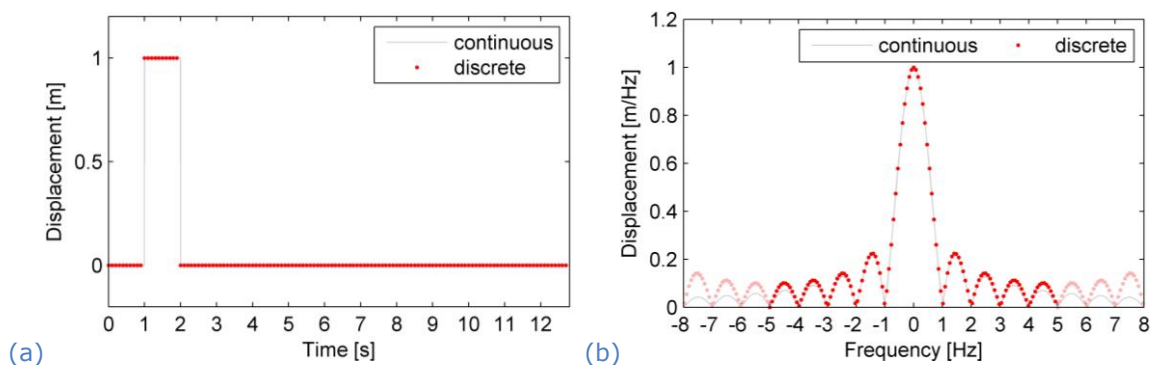


Figure 19: The discrete Fourier transform of a sampled rectangle signal at a sampling frequency of 10 Hz.

Another important error is leakage. This error originates from the fact that measurements have to be taken during a finite observation time. The discrete Fourier transform then assumes that the observed signal is periodic in time with a period the same as the measurement time. If this condition is not met, a leakage error occurs. In Figure 20.a, the harmonic signal of 1 Hz frequency is periodic in the observation window of 3s. All frequencies are zeros except for the fundamental frequency (Figure 20.b). In Figure 20.c, the recorded signal is not periodic within the observation window of 3.5s. As a result, the discrete spectrum does not coincide with the exact fundamental frequency of 1 Hz. Instead, the energy is spread (leaked) to nearby periodic frequencies causing an important amplitude error. This error is a function of the degree of non-periodicity. In the time domain the non-periodicity of the signal within the observation window cause discontinuity and the assumed periodic signal differs from the exact signal. Hence, errors can be expected. This simple harmonic example illustrates the leakage phenomenon. Since any signal can be expressed as a linear combination of sines and cosines, leakage will occur whenever a signal contains non-periodicity frequency components.

The only solution to the leakage problem is to make sure that the signal is periodic or completely recorded within the observation window. Generally, this is very difficult to achieve. The measurement duration has an important influence on reducing leakage, as

shown in Figure 21. If the measurement time of a sinusoidal signal of 1 Hz frequency increases from 3.5s (Figure 21.a) to 6.5s (Figure 21.c), the frequency content shows better accuracy (Figures 21.b and 21.d).

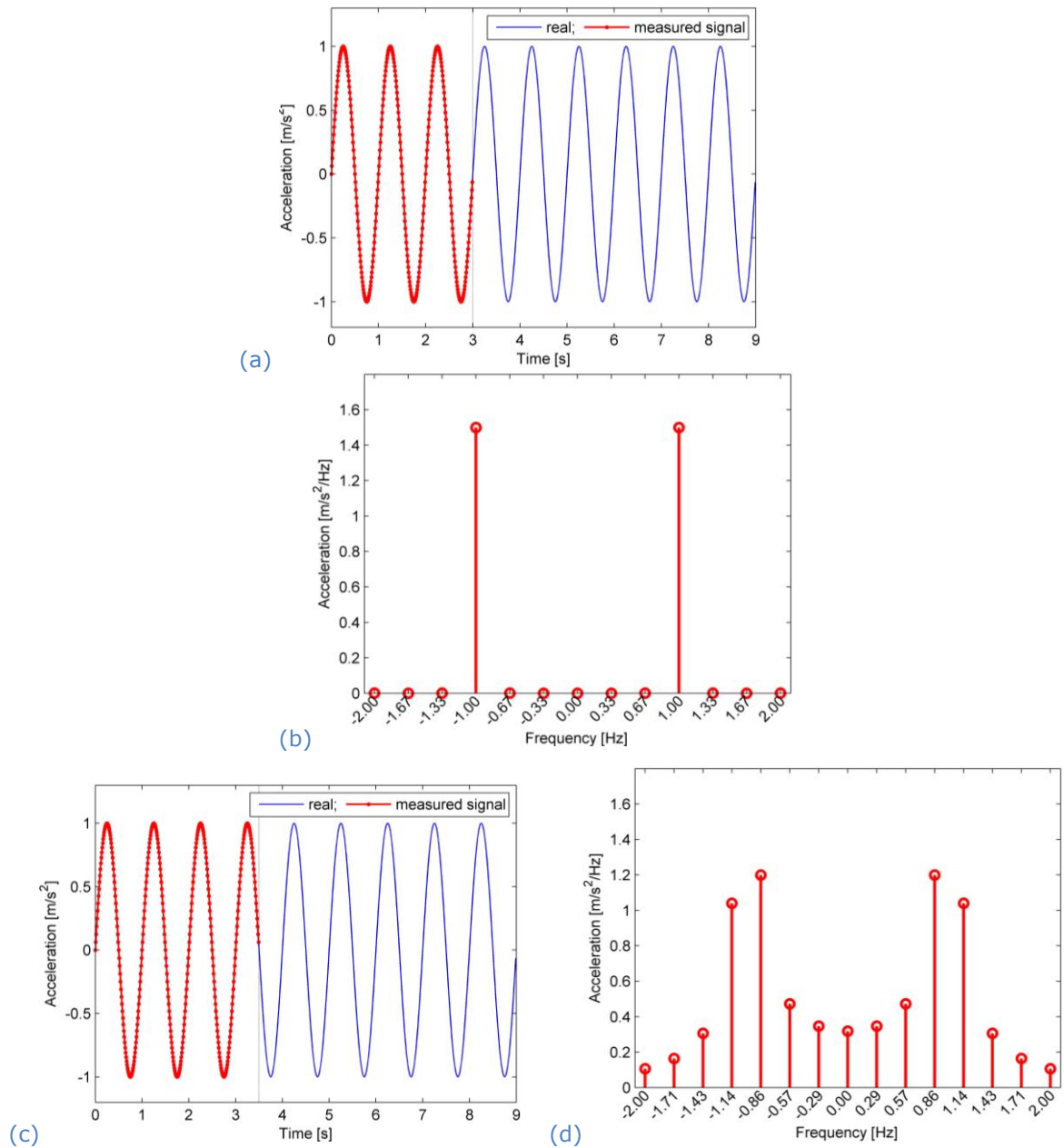


Figure 20: Leakage error due to non-periodicity when measuring a sinusoidal signal of 1 Hz; (a) sampling duration of 3s; (b) frequency content; (c) sampling duration of 3.5s; (d) frequency content.

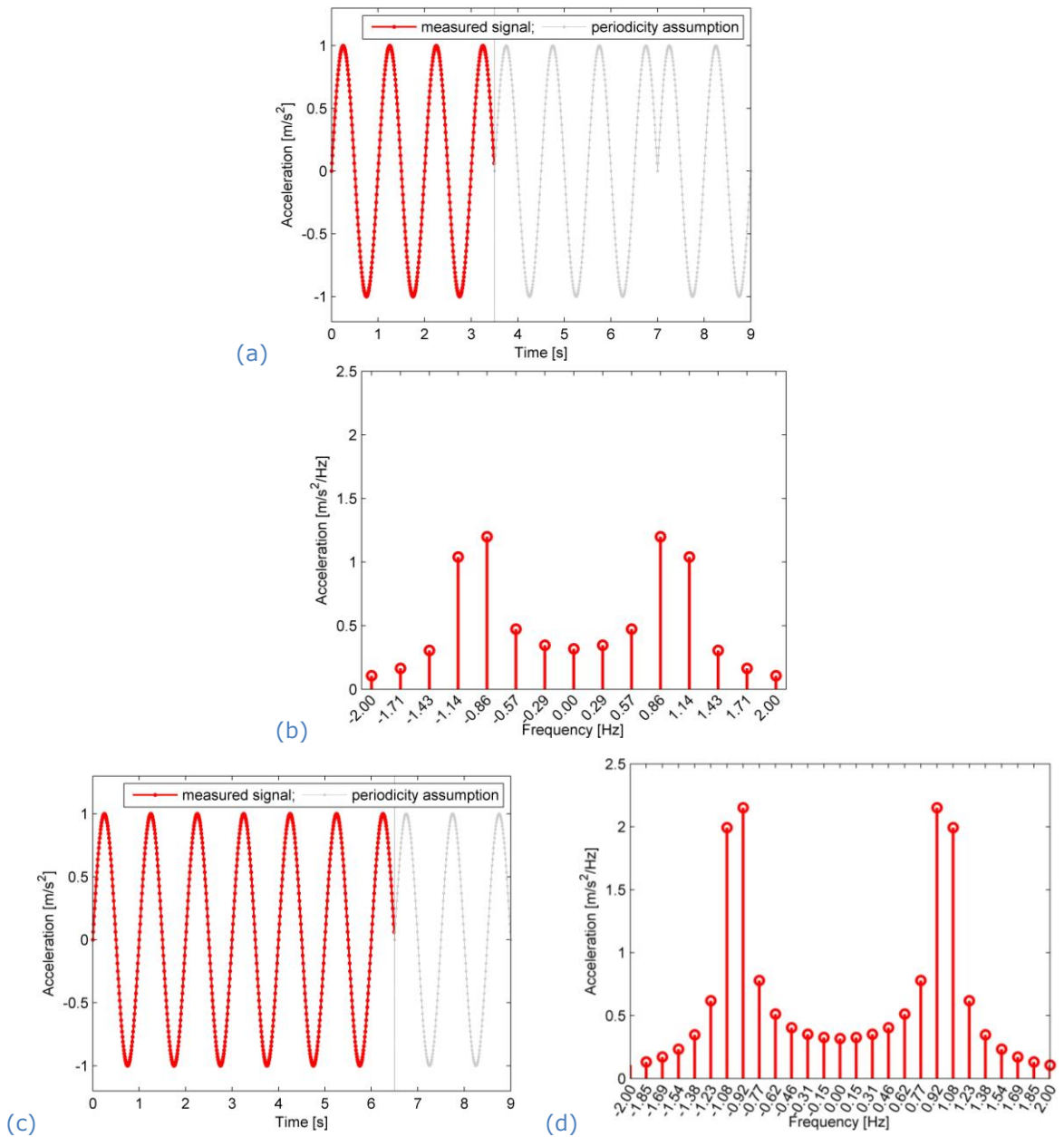


Figure 21: The effect of measurement length on leakage error; (a) Measurement duration of 3.5s; (b) frequency content; (c) Measurement duration of 6.5s; (d) corresponding frequency content.

6.2 Determination of dynamic characteristics

The dynamic characteristics (modal parameters) of a structure can be described by modes, which include natural frequency, damping ratio and mode shape. These modes can be identified from physical, measurable quantities such as acceleration, velocity, strain, etc. with acceptable accuracy and under natural (free) and/or forced excitation sources.

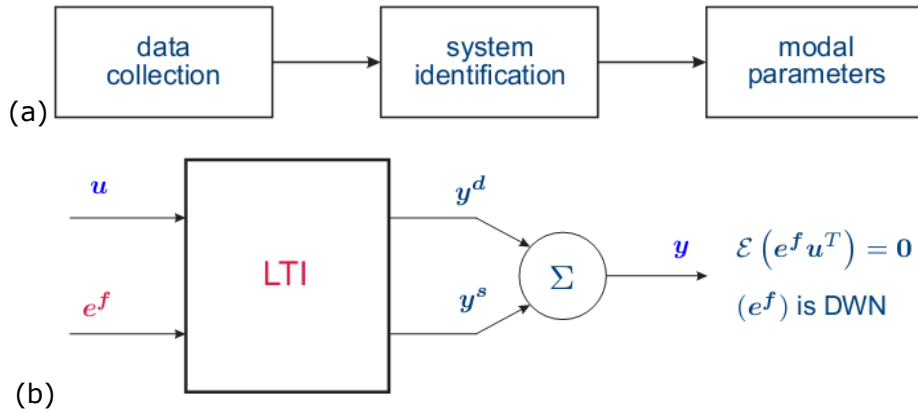


Figure 22: Basics of modal testing. (a) Modal parameters cannot be measured directly; (b) Modal parameters can be derived from the (linear time invariant) model of the identified structure.

After collecting time history data, modal parameters are extracted in a two-step procedure (Figure 22). In the first step (system identification), a model of the structure is identified, e.g. a state-space model or a non-parametric frequency response function. In the second step (modal analysis), the modal parameters of the identified model are calculated and divided into true (physical) modes and spurious modes, that appear due to measurement noise, modelling errors, harmonics, etc.

6.2.1 System identification

In a system identification model, the input in a forced vibration test (FVT) is the information on the excitation side, which is measured. All deterministic system identification methods can be applied in a force vibration test. If input is unknown such as in an ambient vibration test (AVT), the identification proceeds with the fact that no information on the excitation side is measured. This lack of input is translated into a stochastic dynamic load description with mean value equals to zero. And the frequency content of the loading is supposed to be equally distributed over the frequency range of interest. The latter is known as white noise assumption. Amplitude is apparently unknown. The white noise is valid for most kind of ambient excitation except when there is harmonic loading component. Under the white noise description, the forces at different time instances are uncorrelated. This process of identifying the modal parameters of the buildings on operational condition is often called Operational Modal Analysis or OMA.

The output is the measured structural response due to the input excitation as well as the ever present ambient sources such as wind or micro seismicity. The positive power spectra density (PSD) of the measured output signals is defined as the Fourier transform of the positive correlation functions.

The frequency response function (FRF) is defined as a transfer function in which the complex Laplace variable is restricted to purely imaginary values. The practical relevance of the FRF lies in the fact that it is easily computed from the measured time data and we can apply classical input-output modal analysis approaches such as the peak picking (PP) and the complex mode indication function (CMIF).

The peak picking method, as the name suggests, identifies the modal parameters by figuratively selecting the peaks of the averaged normalized PSD function plot. Mathematically speaking, it depends on the modal decomposition properties of the FRF. Similarly, the CMIF method selects the peaks of the function-of-frequency plot (Shih, Tsuei, Allemang, & Brown, 1988). CMIF was originally intended as a tool to count the number of modes that present in the recorded data. As a useful by-product, CMIF also identifies the modal parameters from the frequency response function by selecting peaks of the singular values. This function is the singular values of the identified FRF matrix. Since for the case of AVT with unknown excitation, the FRF is replaced by the sum of the identified positive PSD. Therefore, sometimes it is referred to as frequency domain decomposition or FDD.

These two approaches usually yield rather rough estimates and are often referred to as nonparametric methods. PP is physically intuitive but often fails when structure has closely spaced modes and when modes are not weakly damped. The accuracy of natural frequency is determined by frequency resolution. The damping calculated by half power bandwidth is unreliable. FDD is in fact an extension of PP with improvement in mode multiplicity separation.

Later development into so-called parametric methods often goes through all the about processes. Parametric methods are based on a model. The most convenient way to model a vibrating structure is to rearrange the discretized equation of motions into a state-space model.

$$\begin{aligned}x_{k+1} &= Ax_k + Bu_k + w_k \\y_k &= cx_k + Du_k + v_k\end{aligned}$$

where u is the input vector, y is the output vector and x is the state vector; w and v are noises due to modelling and measurement inaccuracies, respectively; A , B , C and D are state matrices. This state-space equation has an exact solution in the free vibration case. If it is an ambient vibration test, both excitation input and noise are unknown. From a mathematical point of view, it is impossible to differentiate between those terms. Therefore, the input u can be included in the noise term and a stochastic state-space model can be derived.

The covariance-driven stochastic subspace identification (SSI-cov) is developed by identifying the system matrix from output-only data with the assumption of white noise (Reynders, Pintelon, & De Roeck, 2008a). Once the output correlation function is calculated, it can be mathematically decomposed (using single-value decomposition or SVD). Knowledge of the system matrices suffices to estimate modal parameters of frequency f_i , damping ratio ξ_i and mode shape φ_i . In system identification parlance, SSI-cov method is often called stochastic realization. The subspace identification method can be considered as an extension of system realization where direct computation of correlation is replaced by geometrical projection (Peeters & De Roeck, 1999). In fact, the notions of covariance and projection are closely related, because they both aim at cancelling out the uncorrelated noise. Subspace identification is more flexible than realization as it makes the combination of measured and unmeasured loads possible (Reynders & De Roeck, 2008). In the practice of AVT, the subspace identification is purely based on treatment of measured time instants and specifically named data-driven stochastic subspace identification or SSI-data.

Another popular parametric method in AVT is the (stochastic) poly-reference least squares complex frequency domain (pLSCF), which is also known by its commercial name PolyMAX. In fact, it is the most simple yet efficient method for prediction error minimization. The main advantage of this method is to recognize spurious modes due to over-modelling.

A new technique is to supplement the inherently present ambient excitation with a relatively small artificial excitation, like a hammer or a drop weight impact or a force generated by a pneumatic mechanical muscle. A possibility could also be to make use of measured displacements, velocities, and/or accelerations at the supports, as already sometimes done in case of earthquakes. This hybrid technique is called OMAX (Operational Modal Analysis with eXogenous inputs). In the subsequent system identification, the combined (unknown) stochastic and (measured) deterministic force inputs are taken into account (Reynders & De Roeck, 2008). Main advantages, as compared to OMA testing, are more accurately identified mode shapes, extension of the useful frequency interval and possibility to obtain absolute scaling of the modes that are excited by the small artificial forces. As already mentioned, this can lead to a better resolution in the later damage identification process.

In summary, parametric methods are less intuitive than PP and CMIF but they are more consistent. Moreover, they can deal with closely spaced modes as well as highly damped modes. In stochastic identification, pLSCF is less accurate than SSI methods. SSI-cov and SSI-data are of almost the same accuracy. They are both non-iterative method and can be implemented into a robust reference-based version. Interestingly, the statistical accuracy (covariances) of (A,C) can also be evaluated. The subspace identification is more flexible as it allows combination of measured and unmeasured loads. All the above discussed dynamic system identification methods have been implemented in a MATLAB toolbox for experimental and operational modal analysis (MACEC) at the Department of Civil Engineering, KU Leuven ((Reynders, Schevenels, & De Roeck, 2011)).

6.2.2 Deriving modal parameters

A handy tool for finding the correct physical poles of the structure is the so called stabilization diagram, showing the 'stability' of poles at increasing model orders. If model order is higher than the true system order, also the noise is modelled, but the mathematical poles that arise in this way are different for different model orders if the noise is purely white. So, the true (physical) system poles can be detected by comparing the modal parameters for different model orders. In this way, also weakly excited system poles, that appear only at high model orders, can be detected.

In case the noise is coloured, there could exist noise poles that show up at the same frequency for different orders in the stabilization diagram. However, due to their high damping ratios or to the corresponding complex or unrealistic mode shapes, they can be separated from the true system poles. It is also important to select the system poles at a sufficiently high model order, for which the system and noise dynamics have been decoupled. So to clear out the stabilization diagram, for a certain model order, when comparing with the poles of the lower model order, only those poles for which the relative difference in eigenfrequency, damping ratio and MAC value is below a threshold value, are presented (Reynders, Pintelon, & De Roeck, 2008).

However, the stabilization diagram can still show some mathematical poles, especially for high model orders. This prevents not only the full automation of analysis, but also can it make the selection of the physical poles from the stabilization diagram a time consuming step. For this reason an extra criterion – the modal transfer norm, adopted from model reduction theory, is introduced into the stabilization diagram in order to facilitate the full automation of both FVT and AVT with subspace identification methods [(Reynders, Schevenels, & De Roeck, MACEC 3.2: a Matlab toolbox for experimental and operational modal analysis, user's manual, Report BWM, 2011), (Reynders, Houbrechts, & De Roeck, Fully automated (operational) modal analysis, 2012)].

6.3 Interpretation methods

6.3.1 Finite element (FE) model updating

Structural analysis is commonly performed with the finite element (FE) method. This computer model simulates the physical behaviour of the structure and can be used to predict the responses to service and seismic loads, to assess the structural integrity and to study the impact of suitable design modifications. Even with the great advances in the field of structural modelling, an initial FE model is often a poor representation of the actual structure – particularly in the field of structural dynamics – because of a number of simplifying assumptions that depend on engineering judgment. It is generally assumed that experimental vibration data, obtained from dynamic tests, are a better reflection of how the structure behaves than the predictions from the initial FE model, despite the presence of experimental errors. The FE model is therefore corrected in a model updating procedure in which it is tuned to the experimental vibration data. Most often modal data, such as eigenfrequencies and mode shapes, are used for civil structures since they can be identified from forced and/or ambient vibration tests. An alternative approach in mechanical engineering is to use frequency response functions (FRF).

The FE model updating technique can be used for parameter identification, estimation and damage assessment. The key task is to choose the objective functions for error minimization. There are several different physics based equations that are used as either objective functions or constraints for the model updating, depending upon the parameters that are to be identified and the identification algorithm being used. No matter how they are formulated, objective functions seek to quantify the discrepancy between the model predictions and in-situ measurements or properties.

The structural parameters that can be identified from FE updating process with a baseline measurement data. For the purpose of structural control, a long term monitoring strategy can be adopted and the data can be used to track changes in modal parameters. These changes are related to a change in the structural system, i.e. structural parameters.

6.3.2 Derivation of fragility curves based on experimental modal parameters

Lately, research interest has devoted to incorporating structural dynamic properties into fragility functions [(Boutin, Hans, Ibrahim, & Roussillon, 2005), (Michel, Gueguen, & Causse, 2012), (Bui & De Roeck, 2012)]. Parameters that can be obtained directly from a vibration

based test and site experimental data are rather reliable. This method is perfectly suitable to apply in the low-to-moderate seismic regions, where there is often lack of both information on recent earthquake and ground motion record.

By definition, fragility curves are to represent the probability of the occurrence of a specific damage state to a structure, under a certain level of ground motion shaking. As a result, any phenomena, such as degrading of the structural material properties due to aging or probable damages by various events during the lifetime of the structure could inherently influence the extent of response of the building to any arbitrary excitations in comparison to the original intact state. This is to imply that the fragility curves of a specific structure might not potentially hold their initial configuration and could need upgrading continuously.

Dynamic response of structure under ground motion can be estimated by mode superposition method, which requires the Duhamel integral solution. The accuracy of the eigenfrequencies and mode shapes of the structure as well as the modal participation factors and damping coefficients are of paramount importance.

Building damage functions are often in the form of lognormal distribution (FEMA, 2003). A fragility curve is characterized by a median value of the demand parameter, e.g. spectral displacement that corresponds to the threshold of the damage state and by the standard deviation associated with that damage state. For structural damage, let S_d be the spectral displacement. The probability of being in or exceeding a damage state is calculated as:

$$P[d_s | S_d] = \Phi[\ln(S_d/S_{d,ds}^*)/\beta_{ds}]$$

where $S_{d,ds}^*$ is the median value of spectral displacement at which the structure reaches the threshold of the damage state ds ; β_{ds} is the standard deviation of the natural logarithm of spectral displacement of damage state ds ; and Φ is the standard normal cumulative distribution function.

In popular vulnerability analysis methods, the damage parameters are tight to the interstorey drift (interstorey displacement divided by story height). This may be considered as nominal shear. Given ground motion one can calculate the floor displacement by mode superposition. The drift has to be less than a given value at each damage state. In fact the limit value is specific to each categorized structural system. According to HAZUS Manual, the threshold at pre-code seismic design level of the slight damage state can range from 0.0012 to 0.0048 obtained from pushover analyses.

The total lognormal standard deviation is computed by the combination of different contributors. These include the variability in ground motion β_{GM} , the variability in structural model and the variability in damage threshold. The first source of uncertainty, depending on ground motion itself, is aleatory in nature. The second source of uncertainty can be directly estimated from the measurement results as discussed in Section 5.3. The third source of uncertainty can be further improved with recent effort to have more specific analysis to be carried out. Suppose that these sources of uncertainty are independent then the total standard deviation is delivered by the square root of the sum of component variability squares as mentioned.

In summary, seismic vulnerability assessment methodologies need to specify all sources of uncertainty. The method based on field test is able to quantify systematic uncertainty in both the spectrum displacement side with identified fundamental frequency and in structural model side with the uncertainty bound of the modal parameters. The method is limited to be applicable within the slight damage state until proportional limit. Fortunately, for low-to-moderate seismic regions, the first damage grade is of most important concern. The vibration based test could be further used for related assessment purposes such as updating fragility curve before and after an earthquake event.

7 Soil-structure interaction

7.1 Introduction

In the framework of NERA, ambient noise measurement and forced-vibration tests were performed in the EuroProteas large-scale experimental facility in Euroseistest, Greece. The experimental campaigns aimed at identifying dynamic soil-foundation-structure interaction (SFSI), as well as to develop guidelines for optimal design of forced-vibration tests, according to the Description of Work (DoW).

Details on the prototype structure of EuroProteas are provided in deliverable D6.1, whereas fundamentals of soil-foundation-structure are presented in deliverables D6.1 and D6.2. In this section, the instrumentation scheme used in the forced-vibration experiments in EuroProteas is exploited. Next, the dynamic characteristics of the system are identified using system identification techniques from ambient noise measurements. Finally, response due to forced-vibration is presented in selected control points.

7.2 Instrumentation scheme

A large number (typically more than 70) of various types of instruments were installed in every test in both the foundation-structure and the surrounding soil, to obtain a well-documented 3D set of recording and monitoring of the wave propagation and SFSI due to the vibration of the structure. The general idea presented in (Celebi & Crouse, 2001) was used.

Instrumentation included digital broadband seismometers (CMG-6TD and CMG-40T), triaxial accelerometers (CMG-5TD), borehole accelerometers (CMG-5TB) and Shape Accelerations Arrays (SAA). Instrumentation was made available from SDGEE-AUTH and the Institute of Engineering Seismology and Earthquake Engineering, part of the Earthquake Planning and Protection Organisation (EPPO-ITSAK). All the sensors were connected with external GPS receivers. All the instruments were in continuous recording with sampling rate of 200Hz.

As seen in Figure 23, seismometers were placed on soil surface every 1.5m, up to a distance of 9m from the foundation, in two directions (approximately north-south and east-west). The intermediate distance of 1.5m was chosen such as to be exactly the half-width of the foundation (3m in width), while the distance of the 9m was chosen such as to be three times the foundation width, after which we should see no effects of the structural vibration on the soil, as stated in Gazetas (1983). A downhole array was placed in the borehole in the centre of the foundation, with the lower instrument at 3m depth (one time the foundation width) and the surface instrument at the top of the foundation slab. In addition, a 12m-long Shape-

Acceleration Array instrument (Measurand Inc.) was placed in the 12m-deep borehole at a distance of 0.5m from the east side of the foundation. The instrumentation in the soil covers a volume of 21-by-21-by-12m (due to symmetry) in the NS, EW and vertical directions respectively, around EuroProteas.

The structure itself was instrumented with 8 accelerometers covering all directions, in both foundation and roof (superstructure) slabs. Five accelerometers were placed on the top of the roof slab, the three on the direction of shaking (in-plane) and two at two opposite corners of the roof slab (Figure 23), in order to capture out-of-plane and torsional modes of vibration.

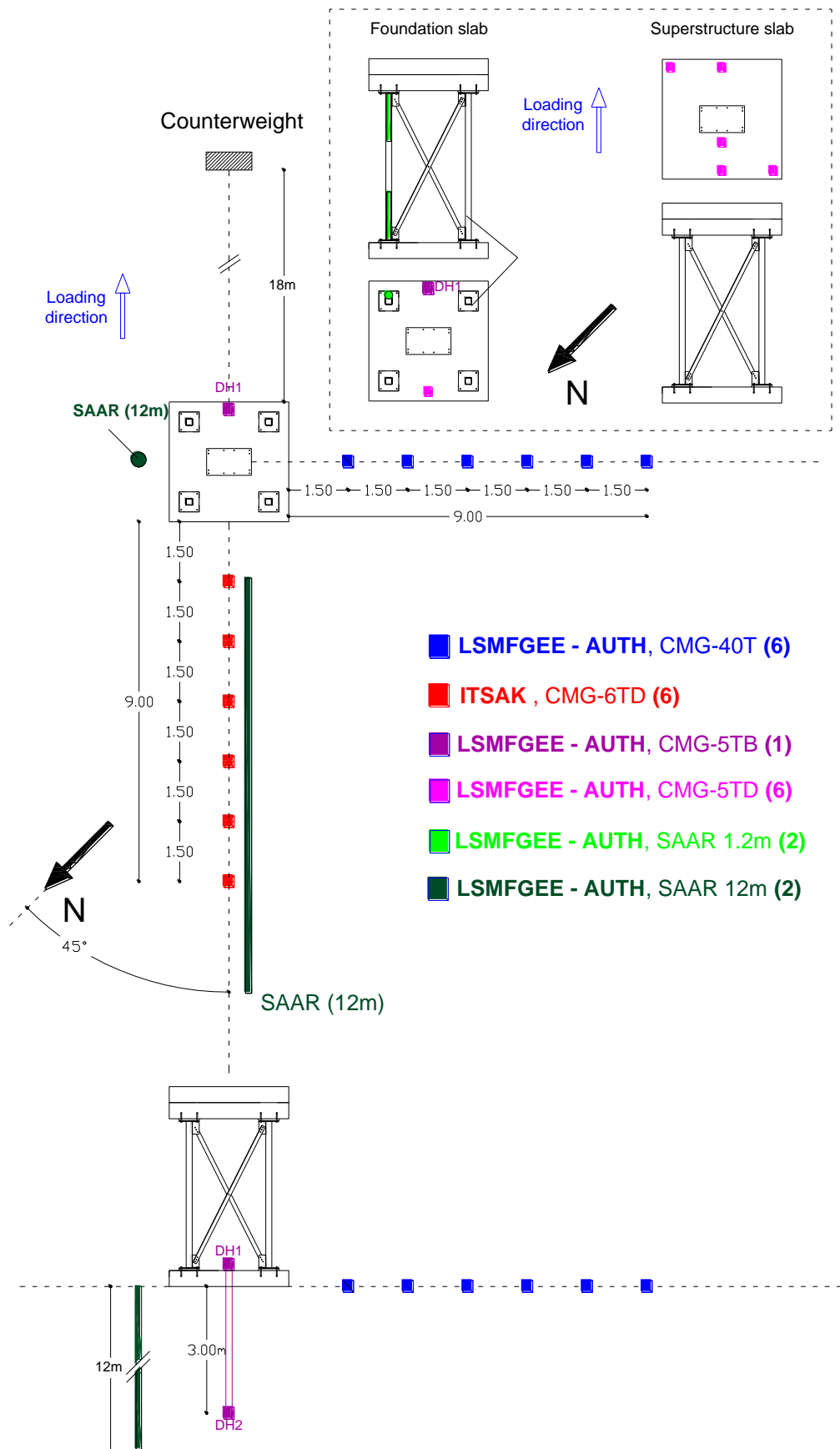


Figure 23: Instrumentation layout of SFSI field tests performed at EuroProteas

7.3 Experimental campaign

The experimental campaign comprised of ambient noise measurements and forced-vibration tests. In total, more than 4 hours of ambient noise was recorded in different seasons (winter, summer) and different times in the day (early morning, noon), while more than 50 intensity levels (and the corresponding frequencies) were exerted in the forced-vibration tests. It is worthy to note that in the forced-vibration tests, the vibrator was placed on the foundation plate as well, in addition to its (typical) placement on the roof slab. The analysis from the performed noise measurements during summer is reported in the following paragraphs.

7.4 Ambient noise measurements

Ambient noise was measured with the full instrumentation setup (Figure 23) in order to identify the dynamic characteristics of the structure and foundation soil, in terms of its resonant frequency and amplification factor. Ambient noise was recorded prior to, and in-between forced-vibration tests, so as to ensure robustness of our results. The frequency and amplification of resonance were determined for both structure and foundation-soil using different types of sensors (Figure 23).

Noise recordings were analysed in the frequency domain using the spectral ratios of horizontal to vertical Fourier amplitude spectra, H/VS (Lermo and Chavez Garcia, 1994). The procedure to compute H/V spectral ratios was the following. Noise windows of 400s duration were selected and divided into smaller windows of 40s duration with 50% overlapping between the adjacent windows. Each window (total number 39) was 10% cosine-tapered and Fourier transformed, and their amplitude spectra smoothed using a Hanning filter. The transfer function of each window was calculated, as well as their average. The coordinates of the first maximum peak of the average ratios, correspond to frequency and amplification of resonance.

In Figure 24 is shown the H/V ratios for the instrument T5860, at central axis of the roof slab for the two directions (in-plane "n0" and out-of-plane "e0"). It can be seen that the soil-foundation-structure system resonates at 4.5-5Hz, while there is a second peak at 9.5-10Hz and another two in 20 to 30Hz frequency range. The first peak is attributed to the soil-foundation-structure system fundamental frequency, representing an uncoupled translational vibration mode, while the second one corresponds to a torsional mode. Figure 25 shows the response at instrument T5861, which is at the corner of the roof slab. A strong peak is shown in the H/V ratios at 9.5Hz, which corresponds to the torsional response of the structure.

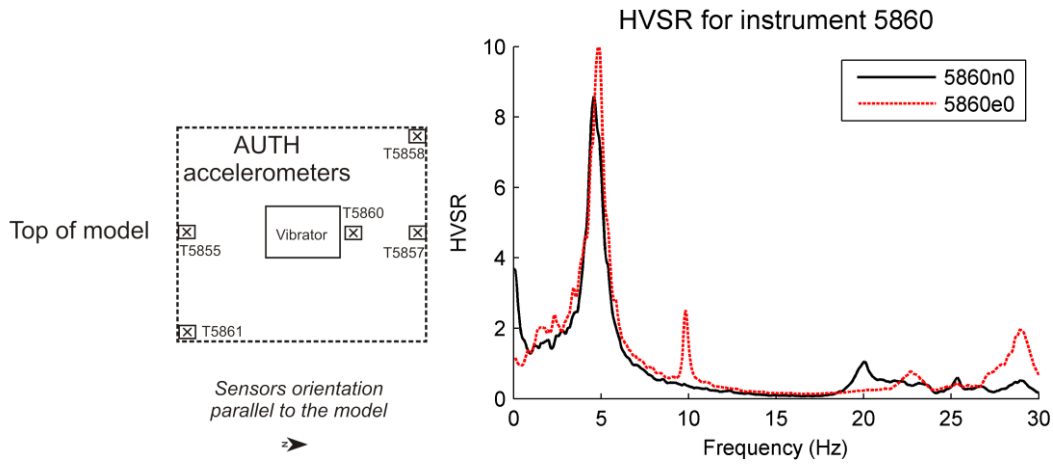


Figure 24: H/V ratios for the instrument T5860 on the roof slab. The instrumentation layout of the roof slab of EuroProteas is also shown.

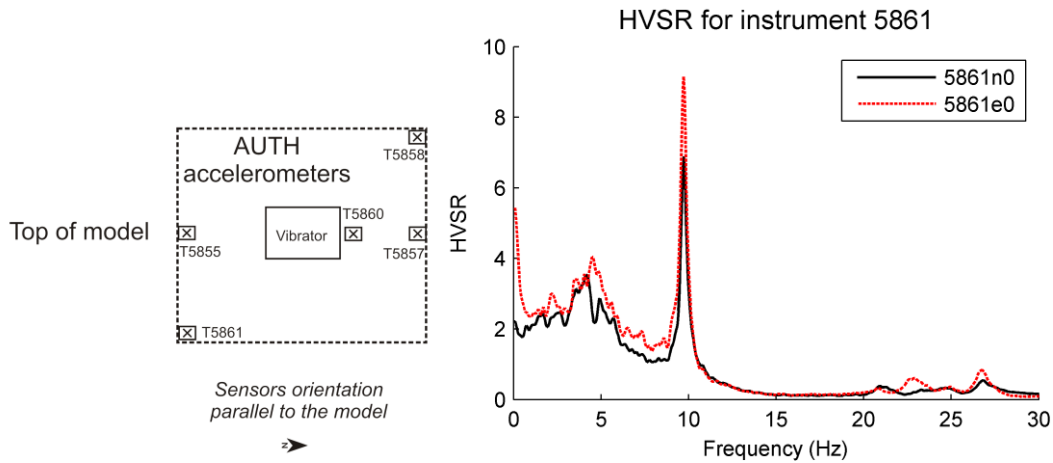


Figure 25: H/V ratios for the instrument T5861 at the corner of the roof slab. The instrumentation layout of the roof slab of EuroProteas is also shown.

Considering the soil, the resonant frequencies of the soil at Euroseistest appear at 0.7Hz, according to (Raptakis, Chávez-García, Makra, & Pitilakis, 2000). In the instruments at distance larger than 6m from the foundation (or two times the foundation width), the resonant frequency is closer to 0.72Hz, which is the resonant frequency of the soil profile at Euroseistest (Figure 26).

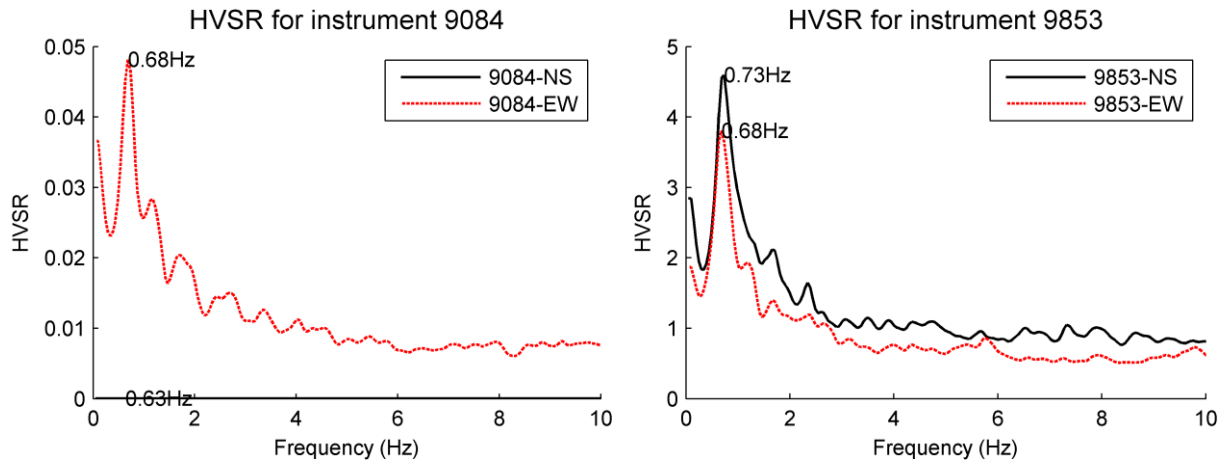


Figure 26: Response at 3m distance from foundation (left) and at 9m from the foundation (right) (instrument 9084 did not perform in the NS direction).

Apart from the HVSR method, system identification was performed for the structure using the software MACEC (Reynders, Schevenels, & De Roeck, 2011), in order to identify the dynamic characteristics of the soil-foundation-structure system of EuroProteas. The model was constructed as shown in Figure 27, where the nodes at the roof slab (at height $z=4.6\text{m}$) are the points of instruments 5858, 5860 and 5861 (Figure 23), where recordings were available.

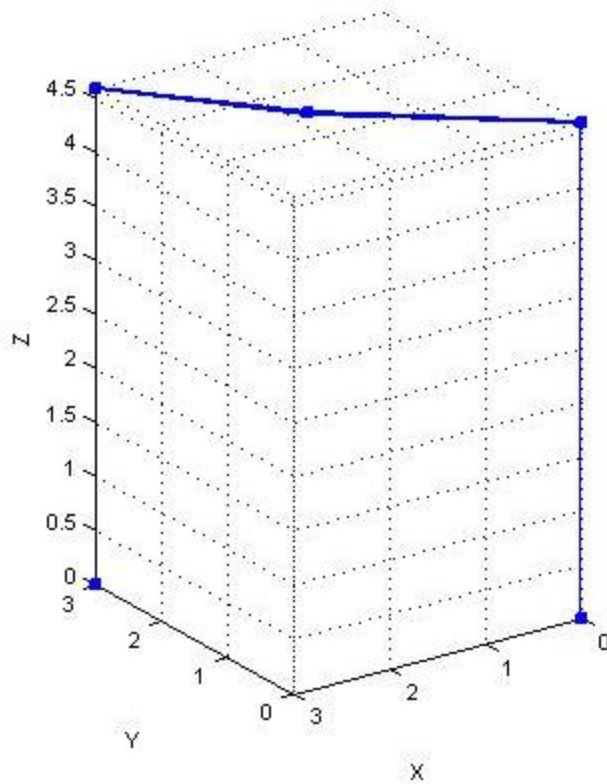


Figure 27: Model configuration in MACEC.

Using the parametric technique of stochastic subspace identification, determination of modal parameters was performed using output-only data. The stabilization diagram in Figure 28 shows the identified stable modes for system order 82. Four modes are identified: two modes at 4.1 and 4.27Hz, representing the two uncoupled translational modes in the two directions (NS and EW) of the model, a clear torsional mode at 9.6Hz and two higher coupled translational-torsional modes at 21.13Hz and 22.45Hz. These resonant frequencies seem to correlate well with the ones produced by the HVSR method, as reported in Figures 24 and 25.

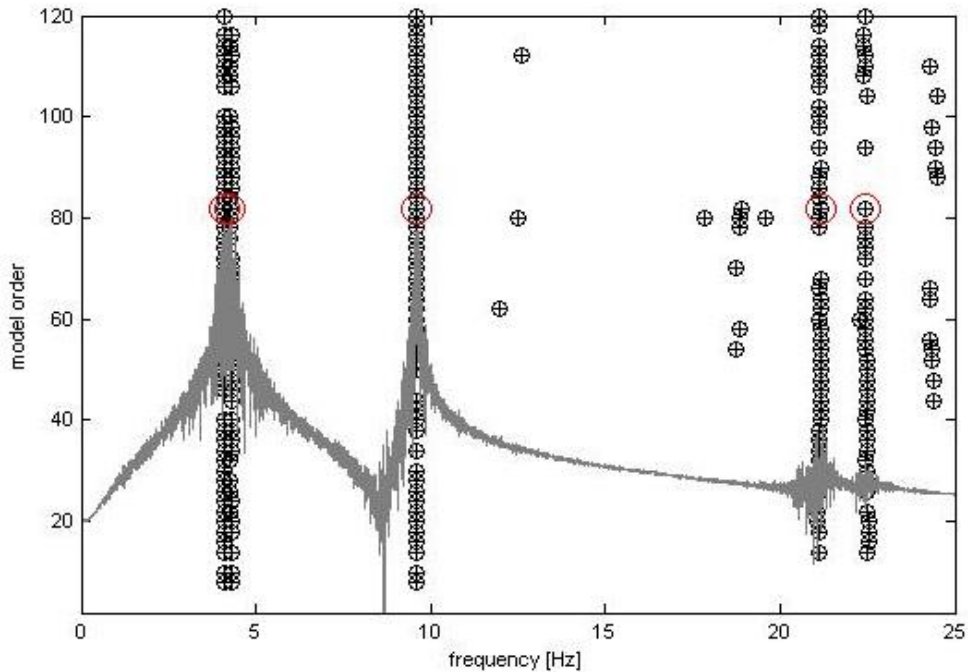


Figure 28: Stabilization diagram of identified modes of EuroProteas.

It is worthy to note that the fundamental frequency of the structure at fixed-base conditions was determined at 8.3Hz, according to the material and geometrical properties of EuroProteas. When accounting for soil-foundation-structure interaction, the resonant frequency of the system shifts down to 4.1Hz, revealing the influence of the compliant soil-foundation system on the dynamic characteristics of the system.

7.5 Forced-vibration measurements

For the forced-vibration tests, the MK-500U eccentric mass vibrator system owned by the Institute of Engineering Seismology and Earthquake Engineering (EPPO-ITSAK) was implemented as a source of harmonic excitation imposed on the model structure. The particular mass vibrator system is a portable, uniaxial dual counter-rotating shaker that can produce a maximum horizontal force of 5 tons and can be operated from 0.1 to 20Hz. The shaker's eccentricity can be varied between 0.15kgm and 11.3kgm in various increments to produce the maximum horizontal force from 10.5Hz to 20Hz. The shaker is powered by a 2.2kW, 1200 rpm electric drive motor (Figure 29.a) controlled by a Toshiba VF-S9 adjustable speed drive. During the forced-vibration tests at EuroProteas, the motor drive was operated manually adjusting the operating speed of the shaker to the desired excitation frequency.

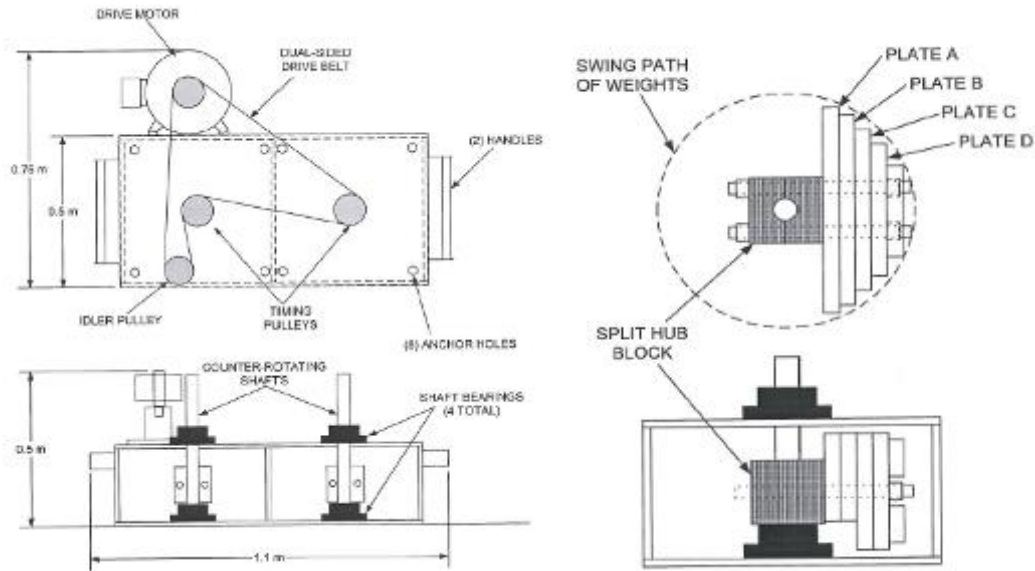


Figure 29: (a) MK-500U schematic (b) Orientation of the mass plates [ANCO Engineers, Inc]

The output force of the vibrator is governed by the following equation:

$$F = E (2 \pi f)^2 \tag{5.1}$$

where F is the shaker output force (in Newtons), E is the total eccentricity of the shaker (in kg-m) and f stands for the rotational speed of the shaker (in Hz). The MK-500U shaker has a total of eight mass plates in four different sizes (A, B, C and D) that can be used to adjust the vibrator's eccentricity (Figure 29.b). One plate of each size is to be mounted to the hub on each rotating shaft in specific order and orientation. These plates allow the shaker eccentricity to be adjusted as mentioned above. Table 1 lists the total eccentricity of the shaker with the mass plates installed and the frequency at which each eccentricity configuration produces the maximum force.

Table 1: 500U shaker eccentricity and maximum operating frequency

Plate	Total eccentricity (kg-m)	Max. (Hz)	Frequency	Force at frequency (ton)	Max.
Rods only	0.15	20		0.24	
A	1.85	20		2.97	
A+B	3.93	17.8		5	
A+B+C	6.93	13.4		5	

The shaker was configured to operate at a frequency range of 1-10Hz. Four levels of progressively increasing excitation force were tested by implementing mass plates A, A+B and A+B+C and A+B+C+D, increasing accordingly the total eccentricity of the shaker. Based on Equation (5.1), the relationship between output force and frequency of the shaker is plotted in Figure 30 for the prescribed mass plate configurations.

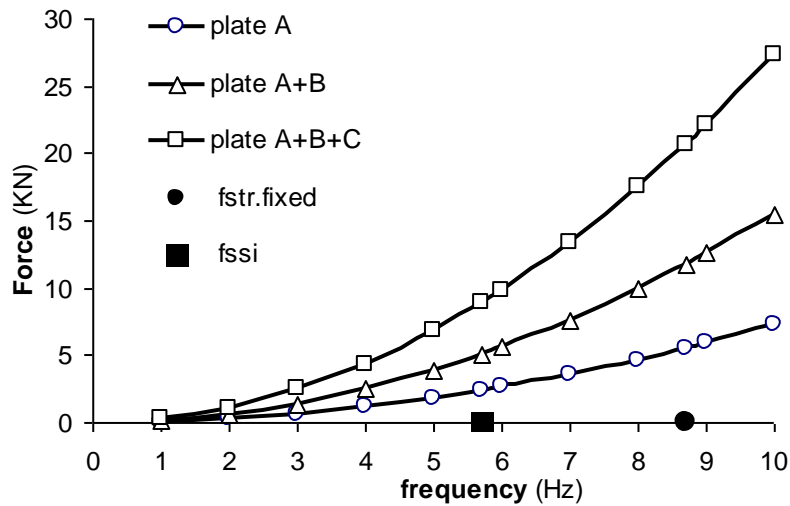


Figure 30: Output force against rotational speed of the shaker for different mass plates configurations

In this series of forced-vibration at EuroProteas, the vibrator was placed both on the foundation and on the top roof slab, in order to increase rocking of the structure.

The recorded response in the instrument T5856 (Figure 23) at different tests is shown in Figure 31, for two plates A+B in the vibrator and for increasing excitation frequency from 2Hz to 9Hz. The scale in the plots is the same, and it is obvious that the response is maximum at around 5Hz.

Forced-vibration Series No. / Mass plate

2 / A+B

Instrument Series No

T5856

Recorded motion

Structural response / Acceleration (m/sec²)

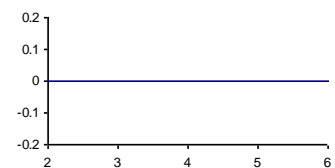
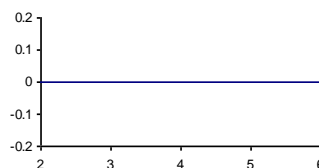
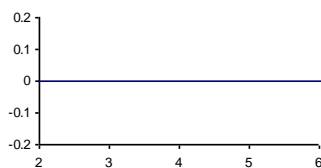
/ f (Hz) / force

EW component

NS component

Z component

14 / 2 / 0.62



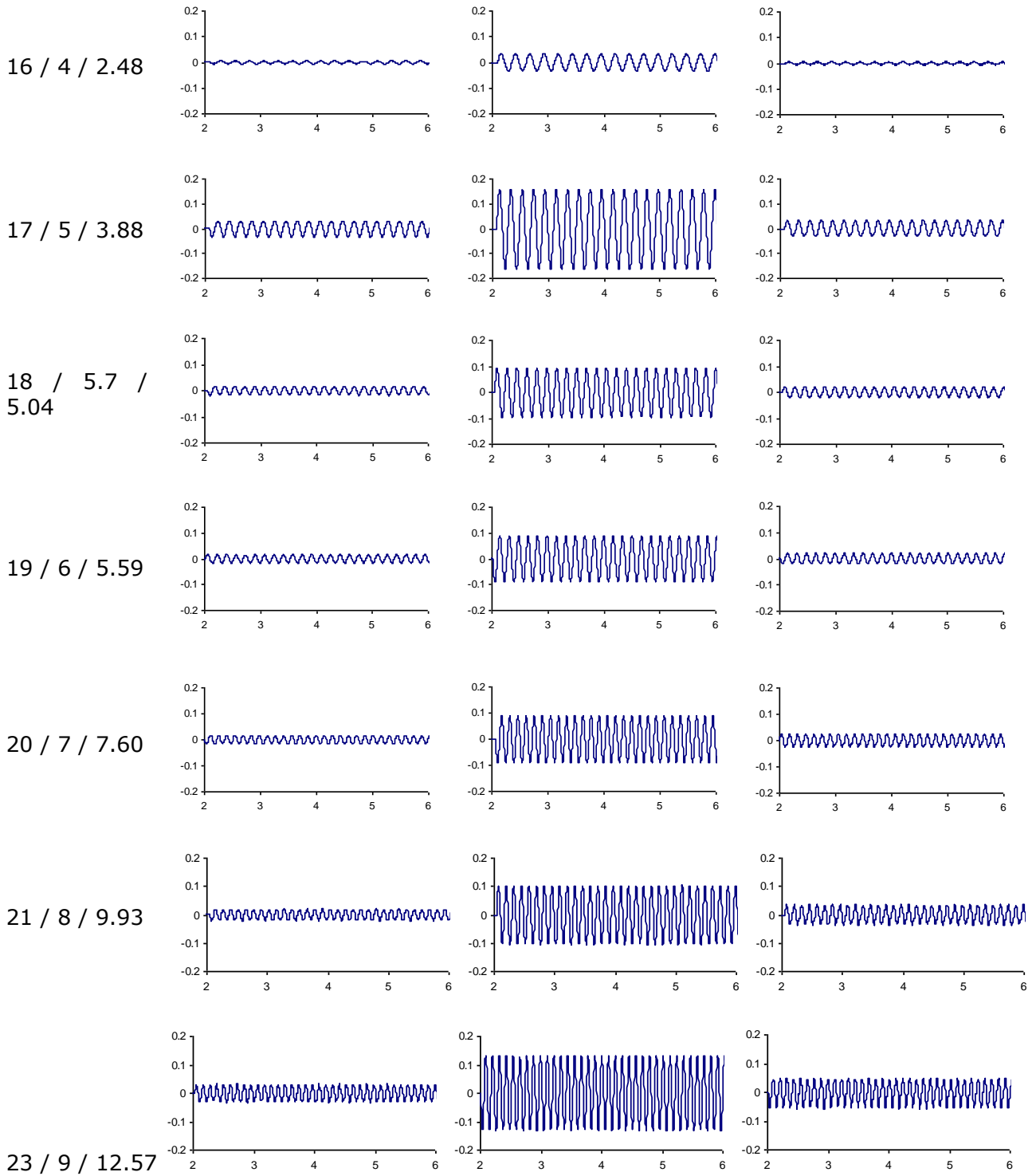


Figure 31: Recorded acceleration response at instrument T5856 for a series of tests according to the output frequency and the output force of the vibrator system.

Response varying with depth is shown in Figure 32, for frequency of the vibrator at 8Hz and three plates, which corresponds to output force of 17.51kN at the roof slab. The response was recorded with the SAAR instruments at every 0.5m. The similar magnitude in the excitation in-plane (x-x) and the out-of-plane (y-y) direction is attributed to the difficulty of orienting the 12m-long instrument in depth.

Forced-vibration Series No. / Mass plate	3 / A+B+C
Test No. / Output frequency (Hz) / Output force (kN)	30 / 8 / 17.51
Recorded motion	Soil response (Vertical)
Type of recorded motion	Acceleration (g)

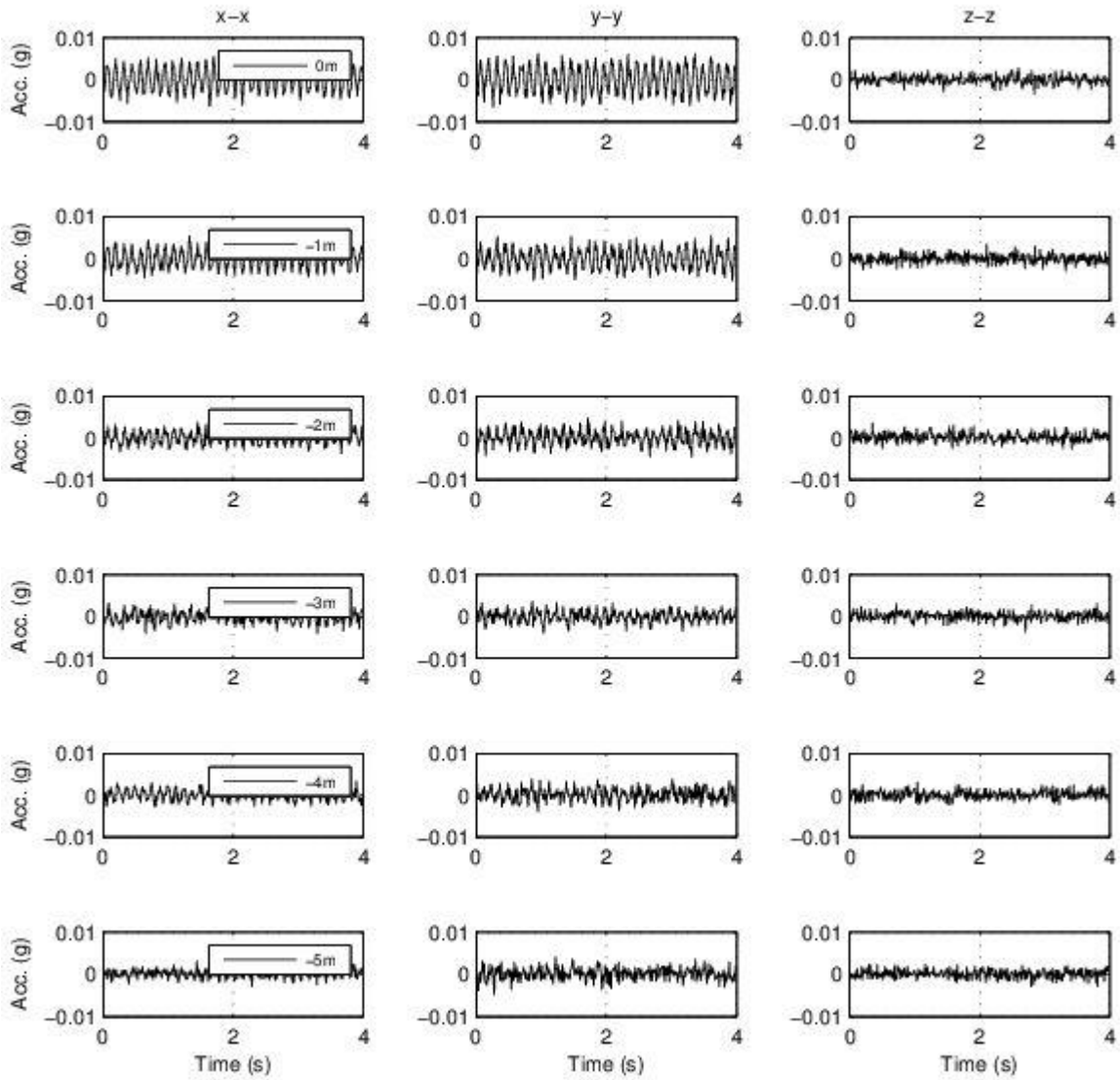


Figure 32: Recorded acceleration in the soil in the vertical array for output frequency 8Hz and output force 17.51kN of the eccentric mass vibrator

Indicative decay of the recorded displacement from the vertical and horizontal SAARs for the corresponding tests can be seen in Figures 33 and 34 respectively.

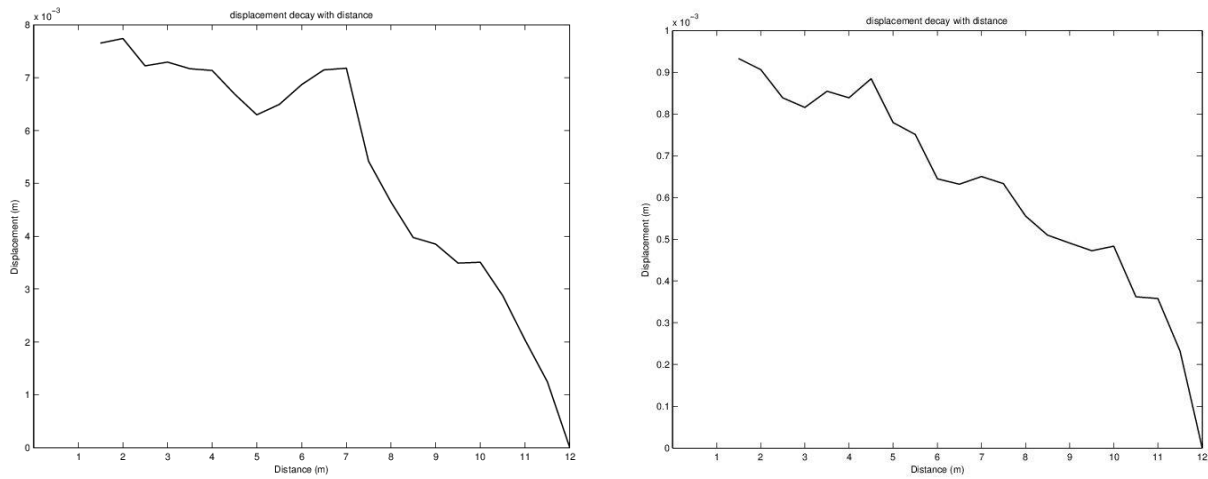


Figure 33: Decay with distance of the recorded horizontal displacement from the vertical and horizontal SAARs for test #18 (output frequency 5.7Hz, output force 5.04kN)

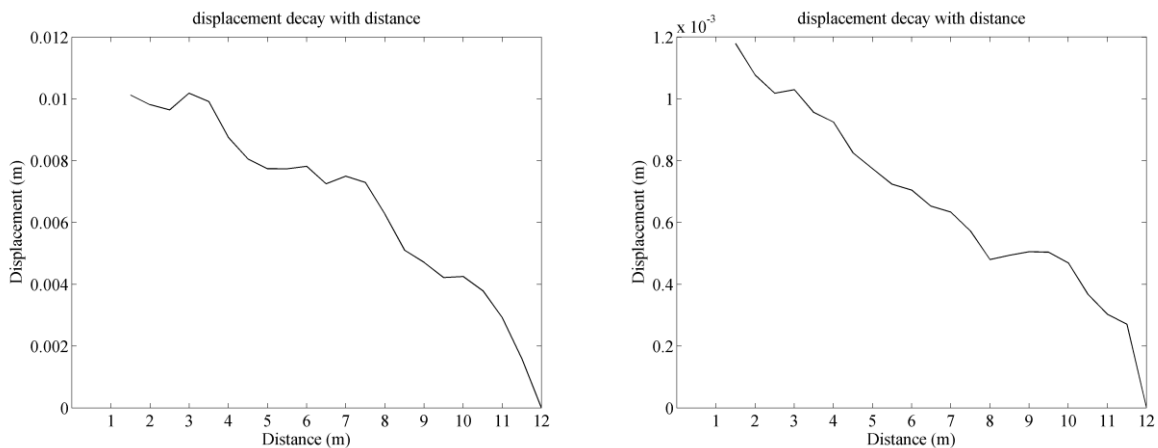


Figure 34: Decay with distance of the recorded horizontal displacement from the vertical and horizontal SAARs for test #30 (output frequency 8Hz, output force 17.51kN)

From the recordings presented above it is clear that the response in the soil beneath the structure is affected by the oscillation of structure, up to a depth of no more than two times the foundation width, for the horizontal mode of vibration. At depth more than two times the foundation width, the soil remains unaffected for practical applications. Moreover, the larger the amplitude of the exciting force, the deeper (naturally) the influence is apparent in the soil. In all experiments, the vertical response in the soil is insignificant, due to the horizontal vibration mode. It would have been interesting to excite the system in the vertical direction (something that could not be performed with the existing equipment) as it is known that in the vertical direction appears the larger stress-bulb beneath the oscillating structure. Nevertheless, for earthquake resistance design of structures, horizontal and rocking vibration modes are usually more important than the vertical one.

7.6 Remarks

Soil-foundation-structure interaction was assessed in large-scale testing facility of Euroseistest, named EuroProteas. The instrumentation of the structure and of the surrounding soil was very dense, in all three directions, in order to capture the full wave propagation phenomenon due to the structural oscillation. Ambient noise measurements and forced-vibration tests were performed to reveal and highlight the importance of soil-foundation-structure interaction in the response of the structure and in wave propagation around in the surrounding soil.

Regarding the field experiments, they require a large number of people to be performed in safety and according to the designed procedure. Contrary to laboratory experiments, field-testing is vulnerable to weather changes (heavy rain, wind, frost, extreme heat), and should be carefully prepared and executed.

Instrumentation has to be designed and placed on both the structure and the soil. In the soil, the instrumentation can be preferably placed at distances from the structure that are fractions of the foundation width, in order to be consistent with numerical and analytical procedures that utilize the foundation half-width or full width as a characteristic dimension. We noticed that for relatively high exciting forced (around 20kN), recording instruments do not need to be placed further than two-three times the foundation width, in both horizontal and vertical arrays.

Due to purely horizontal excitation force, vertical response is insignificant. On the other hand, it is interesting to note that the horizontal stress bulb, or similarly the decay of horizontal displacement, created in the soil due to the structural oscillation, extends in all directions the same, as described in the literature.

Instrumentation on the structure has to be placed in both in-plane and out-of-plane directions of loading, as well as at control points away from the axis of symmetry (if any), in order to capture, apart from the translation, rocking and torsion response. Preferably, the foundation has to be instrumented as well, in order to extract frequency response functions for the structure. The instrumentation scheme at the foundation can follow the one for the superstructure or the roof, for simplified systems such as EuroProteas.

Regarding the level of the force excitation in real-scale experiments, in most cases it is recommended that the structure and the soil behaviour remain in the elastic region. To preserve elastic behaviour during forced-vibration tests, two actions can be executed. First, prior to experiments, extensive numerical and analytical simulations of the system behaviour under forced-vibration have to be performed, in order to investigate the limits of elastic material behaviour for the structure and the soil. Second, prior to and in-between forced-vibration sweep tests, ambient noise vibration measurements can provide with the resonant frequencies of the soil-foundation-structure system. If further shifting down from the established flexible-system fundamental frequency is noticed, most likely nonlinear or inelastic phenomena have occurred. The latter would affect significantly the experimental campaign, as they would imply a completely different system under study.

After the SFSI experiments and pertinent numerical analyses, the parameter that was found to play the most important role for the design of the structure was found to be the relative stiffness of the structure and the soil. More specifically, relatively stiff structures on soft soil are very prominent to soil-foundation-structure interaction. In addition, the mass of the super structure plays important role in the overall seismic response of the system. The larger the mass, the more important are the SFSI effects. These results come to validate the engineering knowledge from past studies documented in the literature.

For horizontal excitation of the structure, the extent of the wave field emanating away from the oscillating structure was found to decrease significantly after two times the width of the foundation, in both horizontal and vertical direction. Unfortunately, we could not perform vertical loading of EuroProteas in order to study the wave propagation around the structure. With the given instrumentation scheme and the specific loading scenarios, it was very difficult to distinguish if soil behaved in a nonlinear way. Given the relatively low amplitude of the excitation force, in all experiments, the soil beneath the structure, as well as the structure, were sought to behave in the linear elastic range.

Concerning the field measuring instruments, the Shape Acceleration Arrays have large noise error (magnitude of approximately 10-4m), which restricts their recording adequacy mainly to large amplitude motions. On the contrary, they prove to be very useful for recording response in an array (in the soil or in the structure), something that cannot be done in this density with conventional seismometers.

On the other hand, accelerometers and seismometers provide excellent means of recording response on the structure and in the soil respectively. In addition, it is very important to have dense instrumentation in the vicinity of the structure, as the response is rapidly decreasing with increasing distance from the foundation.

7.7 Acknowledgements

System identification analyses with MACEC were performed by Sotiria Karapetrou. Achileas Pistolas helped in the ambient noise measurements and interpretation. Their contribution is greatly appreciated.

8 Concluding remarks

These guidelines propose a review of the field forced vibration testing methods giving a short introduction to all the components necessary to carry out these tests. The issues with which to deal in the planning of forced vibration tests are widely explained. The field testing data analysis and the algorithms for the modal characteristics identification are shortly explained. The method to test the soil-foundation-structure interaction is stated.

The guidelines show the higher difficulty to plan an optimal forced vibration test than the one to plan an optimal ambient vibration test. The difficulty increase is due to the right selection of the forcing method and the definition of the force to apply to structure. The increased quality of the results obtained with forced vibration testing methods respect to the ones estimated from the ambient vibration testing methods is showed in the second case study

proposed hereafter. This quality increment of the results does not justify the higher cost of the forced vibration tests in case of a wide campaign of measures to estimate the loss risk of structures and infrastructures in case of natural events. On the other hand forced vibration tests can be useful to assess the vulnerability of strategic structures.

9 Case studies on forced vibration testing

9.1 Industrial building (Seibersdorf, Austria)

The investigated structure is situated in the Austrian highest seismic region and was erected in the year 1979. The main building with an inside radioactive waste combuster and additional machinery complex is surrounded at all edges with building parts at different height levels. The height of the reinforced concrete structure is about 15 meters and due to different foundation and mass distribution it is connected to adjacent structures only with elastic building joints. For consideration the interaction between the different dynamic systems (investigated structure to adjacent building parts and inside machinery complex) a detailed analysis was necessary.

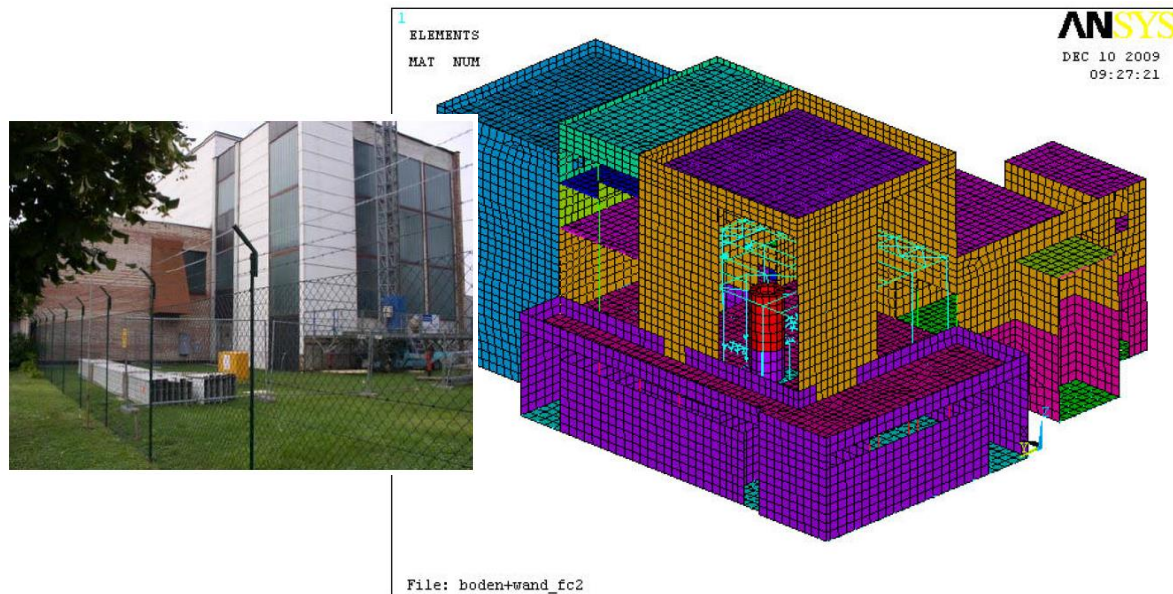


Figure 35: The investigated building in Seibersdorf.

9.1.1 Field testing

In 2009, forced vibration tests were performed on the building using the former AIT's electrohydraulic exciter VICTORIA. The exciter position was positioned in front of the building as seen in Figure 2. Power transmission was realized via a rod chain connecting VICTORIA to the building at an angle of 45° (Figures 36 and 37).

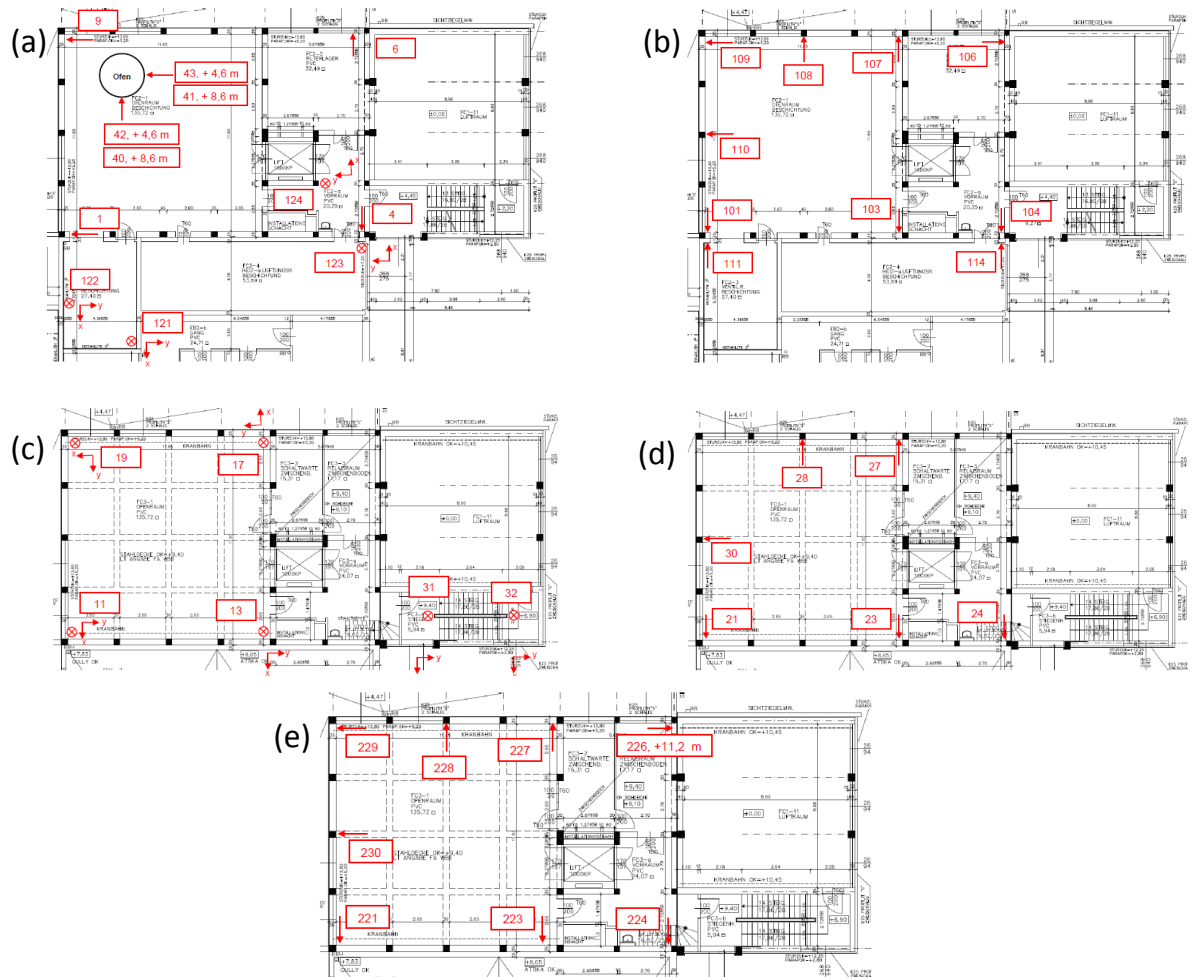


Figure 38: Measurement layout: (a) 1st level (4.6m), (b) 2nd level (7.1m), (c) 3rd level (9.4m), (d) 4th level (9.6m), and (e) 5th level (12.0m).

9.1.2 Data analysis

A modal analysis was performed with the initial step having been the generation of a model grid (Figure 39). In the next step, a transfer function between the excitation point and measurement points was computed. Herein, a complex division of the respective cross spectrum by the power spectrum of excitation is performed. Resulting from this analysis, four mode shapes could be identified within the frequency range 4 to 9 Hz (Table 1).

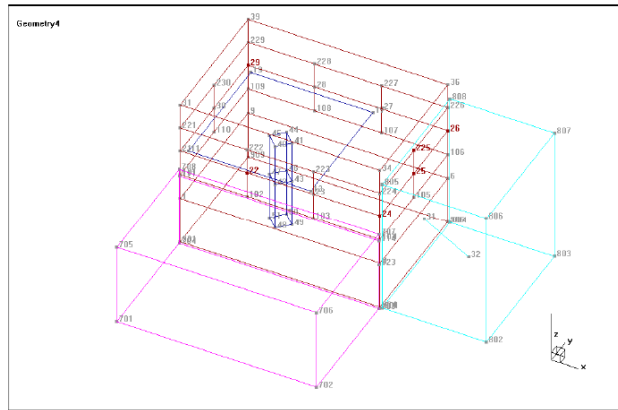


Figure 39: Model grid.

Table 2: Identified modes.

Mode	Frequency (Hz)	Damping (%)
1	4,6	5,1
2	5,6	6,6
3	7,5	5,6
4	8,6	2,7

9.1.3 Numerical analysis

Numerical analysis was performed using a FE model to compare the computed dynamic values with the measured ones. The FE model was calibrated making use of the four identified frequencies in Table 1 as well as via fine-tuning of material parameters (e.g. E-module). The model results are given in Table 2 and Figure 40 (Flesch, Friedl, & Kwapisz, 2011).

Table 3: Comparison of model data and measurement values.

Mode	Frequencies		Deviation in %
	Measurement	Model	
1	4,62	4,65	0,65
2	5,74	5,45	5,05
3	7,39	7,49	1,35
4	8,65	8,54	1,27

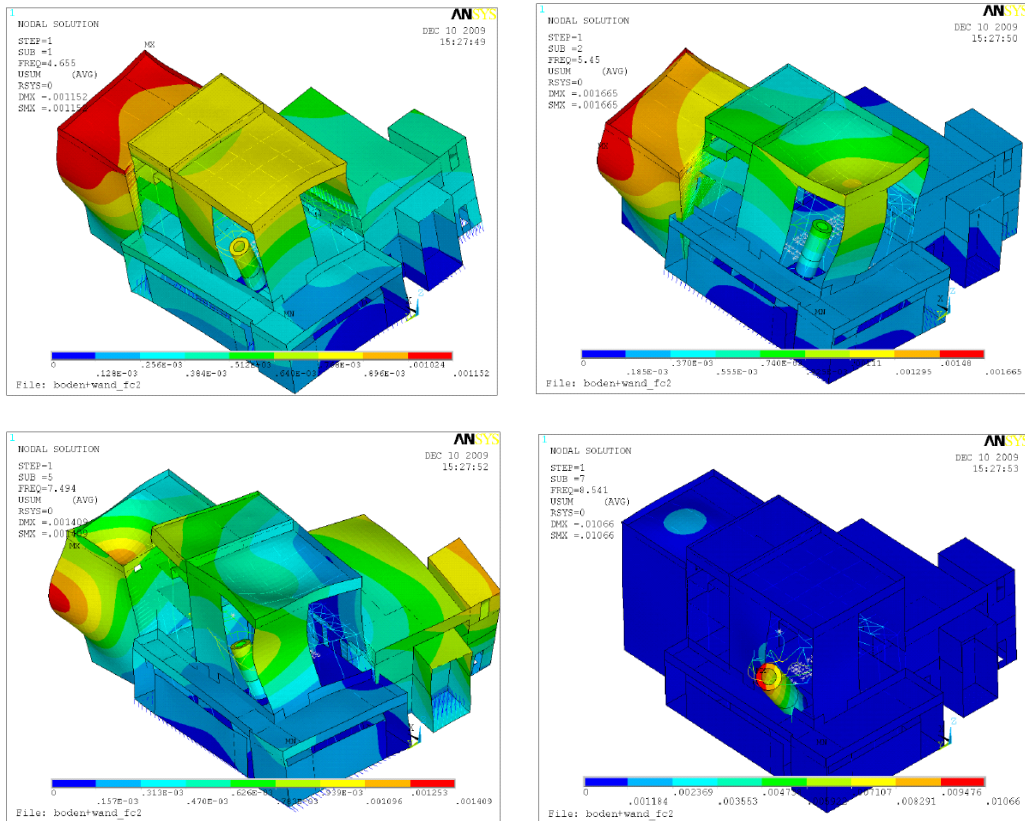


Figure 40: Calibrated FE-models (top left: 1st mode; top right: 2nd mode; bottom left: 3rd mode; bottom right: 4th mode)

9.2 Residential building in Vienna

9.2.1 Structure description

A residential building in Vienna was tested with the AIT's MoSeS on October 2013. This building is a typical unreinforced masonry structure built in the second part of the Wilhelminian time. The structure is composed by two twin buildings linked by the stair case. The two buildings have 4 floors plus an underground floor, as the picture and the drawings in Figure 41 show.

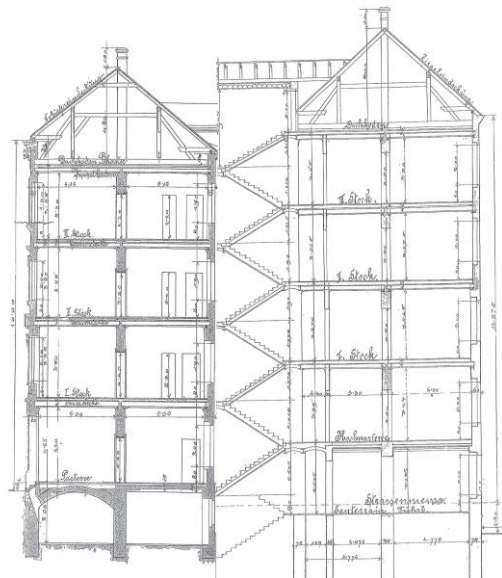
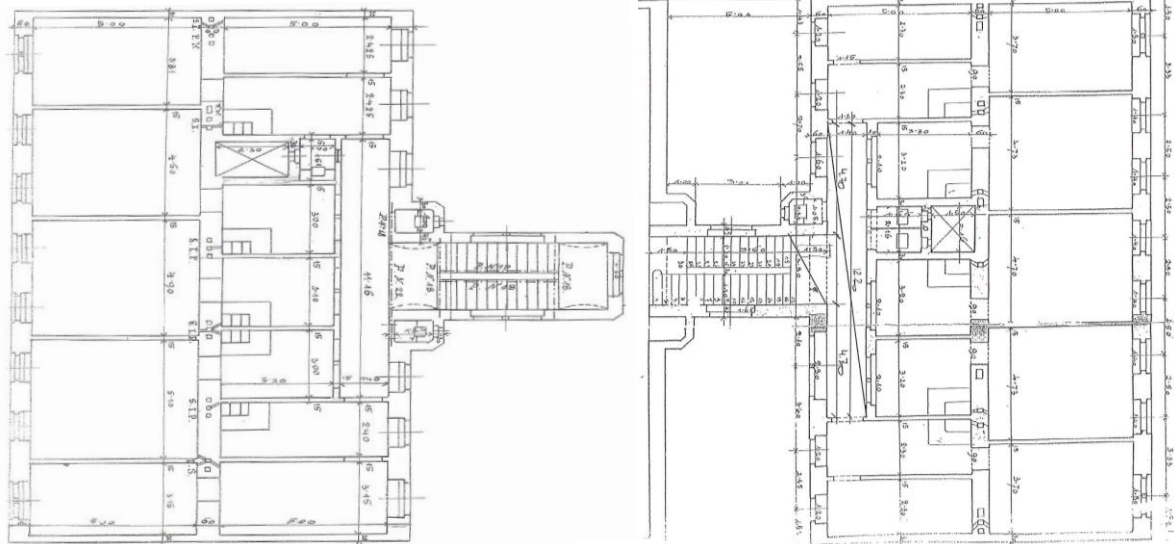


Figure 41: Picture and drawings of the building

9.2.2 Field test

The structure was tested both with ambient vibration method and forced vibration method. The structure was fully accessible, so the sensors could be placed in any part of the structure.

For the forced vibration test the MoSeS truck was parked in front of the building in the street-side and MoSeS was unloaded in front of the building (see Figure 42.a). The rod-chain attached the shaker working on 45° angle to structure and it was anchored to the structure with a steel bar fixed to a window on the second floor (see Figure 43). MoSeS was placed at 30° angle respect to the building façade (Figure 42.b) to excite optimally the first 4 modes of the building. The anchorage height to the building was the highest of the technically possible ones.



(a)



(b)

Figure 42: MoSeS parking



(a)

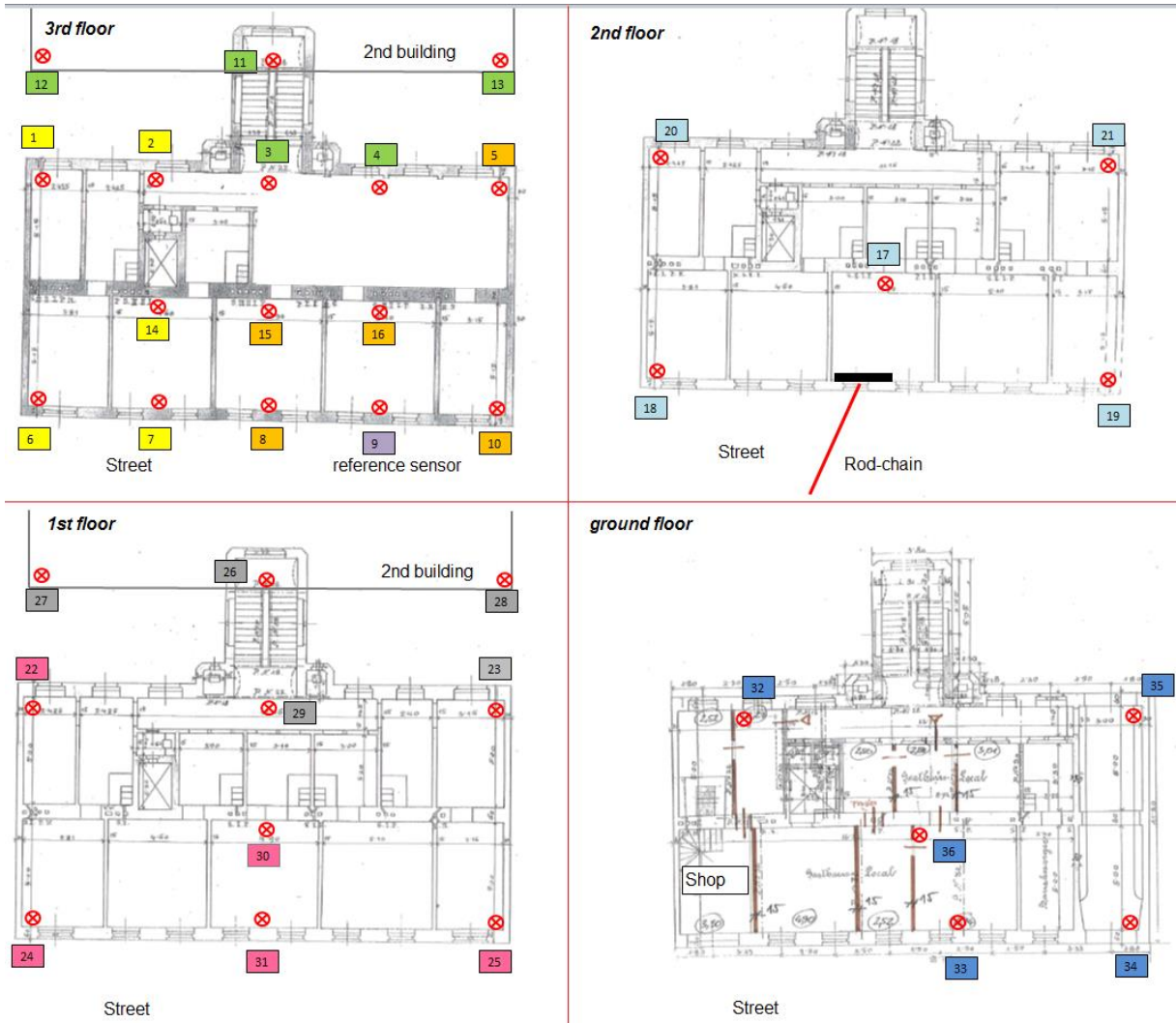


(b)



(c)

Figure 43: MoSeS' attachment to the building. (a) Rod chain positioning (b) Rod chain fastening to the building (c) Rod chain ready.



(a)



(b)

Figure 44: Sensors layout (a). Wired technology of sensors (b)

Eight wired biaxial sensors were used to measure the acceleration in both the horizontal directions. Five different measurement sets were carried out, changing the position of seven sensors and leaving one (sensor 2) in a fix position as reference, as illustrated in Figure 44.a). Due to the wired technology (Figure 44.b) of the sensors used, the measurement layouts were designed considering the practical difficulty to change the position of the sensors and the linking cable for each measurement set, so the sensor were moved in the near positions. The sensors layouts were designed considering that the two twin buildings were linked by the staircase, so complex rotational vibration modes were expected to be among the first ones. The sensors were placed in both the buildings, but in the second building only on the staircase side because of the wires length. Besides the signal dispersion due to the length of the cable, the wired technology affects also the sensor layout because the limited length of the cable. On the other hand measurements with wired technology are possible in all the environments, while the wireless technology could be used only for measurement in environment where nothing could interfere with the signal transmitted by the sensors. In this case the choice of using a wired technology is due to the higher cost of the wireless one that is not justified by higher results quality.

For each sensors layout the ambient vibration test was carried out immediately followed by the forced vibration test. The force applied by the AIT's MoSeS was 2kN and the frequency range excited was 0-20 Hz, so MoSeS was used with the 4 plates configuration (see Figure 45).

		Reference sensor						
Sensor	1	2	3	4	5	6	7	8
Storey	3	3	3	3	2	1	1	Ground
Direction	x, y	x, y	x, y	x, y	x, y	x, y	x, y	x, y
Number of layout								
1	6	9	12	5	18	22	27	32
2	7	9	11	15	20	24	26	33
3	14	9	13	8	17	30	28	36
4	2	9	3	16	19	31	29	35
5	1	9	4	10	21	25	23	34

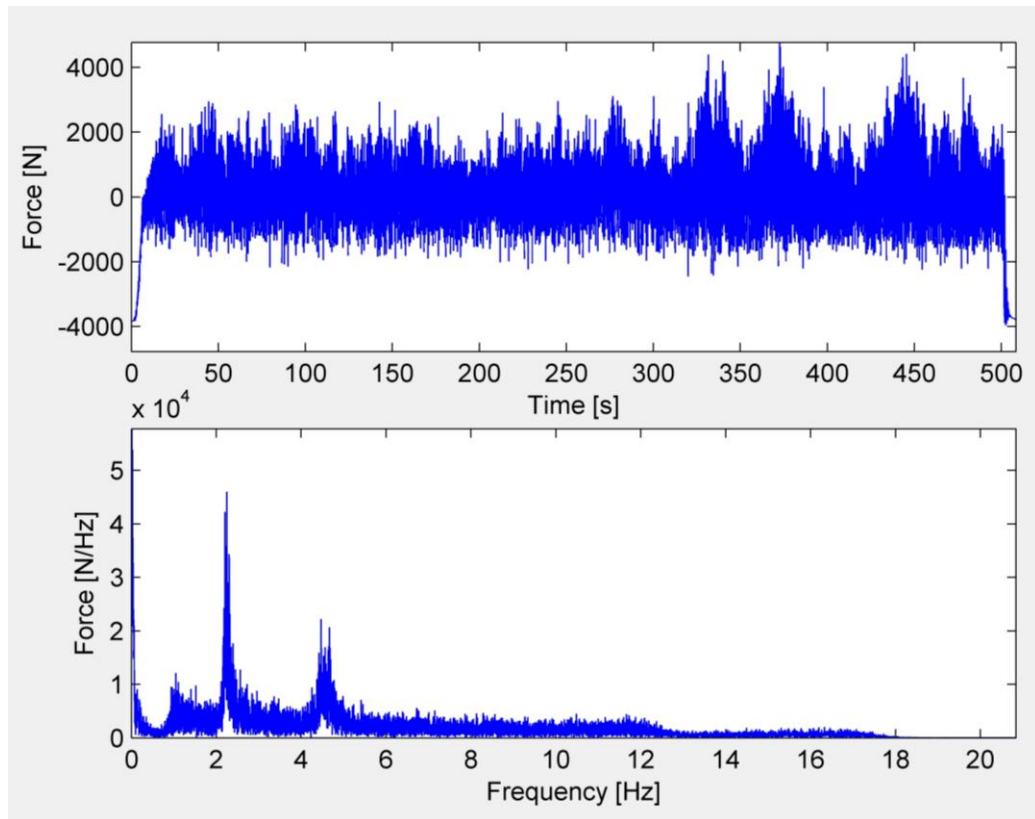


Figure 45: WN applied by MoSeS

9.2.3 Data analysis and results

The signals recorded during both the ambient vibration and the forced vibration test were preprocessed, removing the offset, reducing the signal noise and cutting a frequency range that was interesting for the modal analysis. The data so prepared were analysed and frequencies and mode shapes were identified. The Figure 46 show the signal recorded by sensor 3 in y direction in the first measurement set, i.e. record 12y indicated in Figure 44.a. The Figure 46.a shows the signal of the measuring point 12y recorded in the forced vibration test, while the signal of the same measuring point 12y recorded in the ambient vibration test is presented in Figure 46.b. From the comparison between these two signal records it is plain that the natural frequencies of the building are clearly identifiable in the signal recorded in the forced vibration test. Furthermore the different participation of each vibrational mode is also extremely clear analysing the signal recorded in the forced vibration test differently from the analysis of ambient vibration test data.

The natural frequencies and the mode shapes were identified from the ambient vibration testing data by applying the stochastic subspace method. The first 4 natural frequencies and damping ratios identified are listed in the Table 4, while the Figure 47 shows the first 2 identified mode shapes.

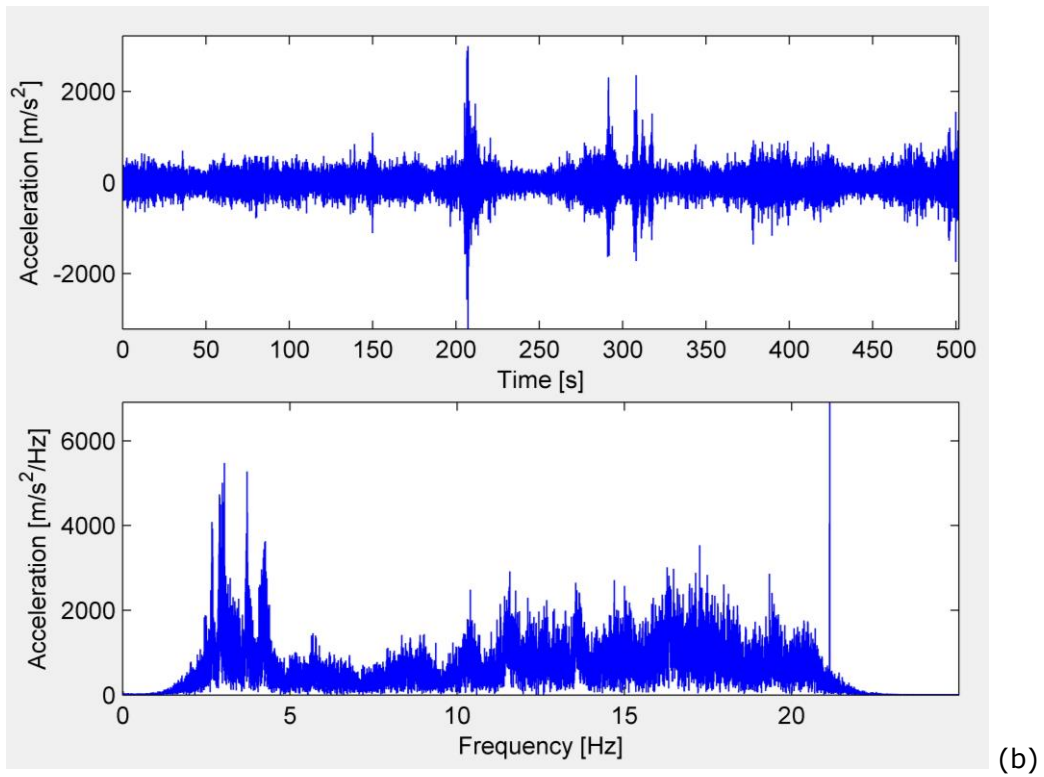
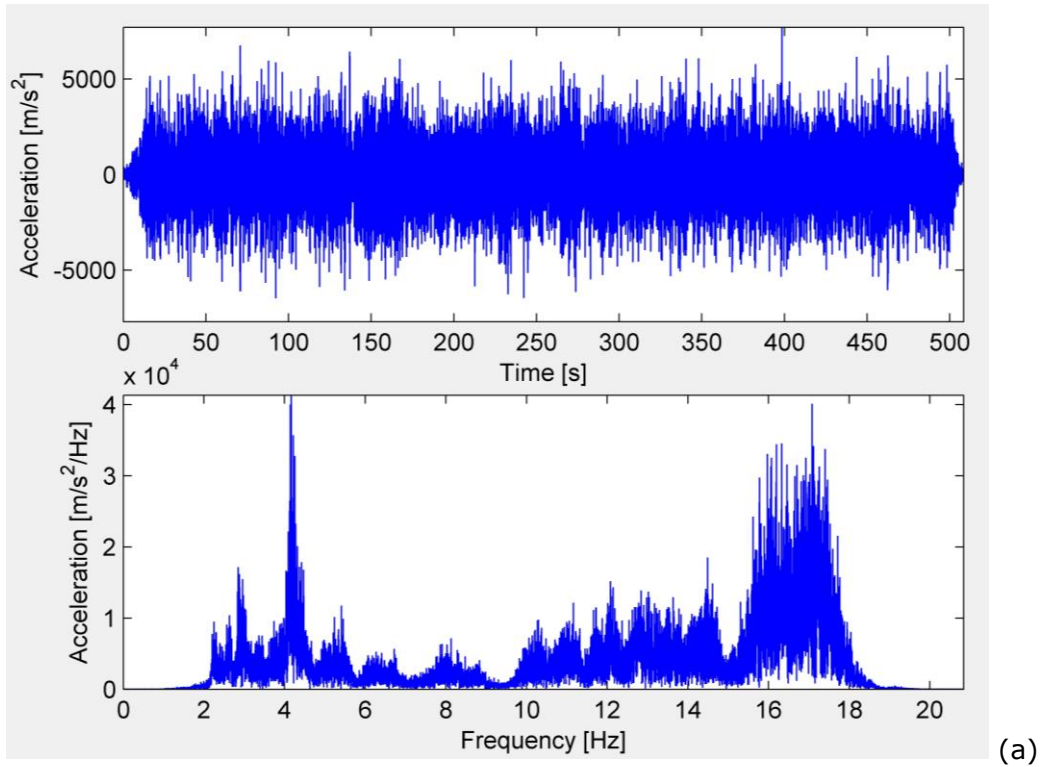


Figure 46: Signal recorded in the measuring point 12y a) in the forced vibration test and b) in the ambient vibration test.

Vibrational mode	Natural Frequency [Hz]	Damping ratio [%]
1	2.91	6.03
2	4.25	5.70
3	7.20	4.94
4	9.84	3.09

Table 4: Natural frequencies and damping ratios of the structure from the ambient vibration testing data

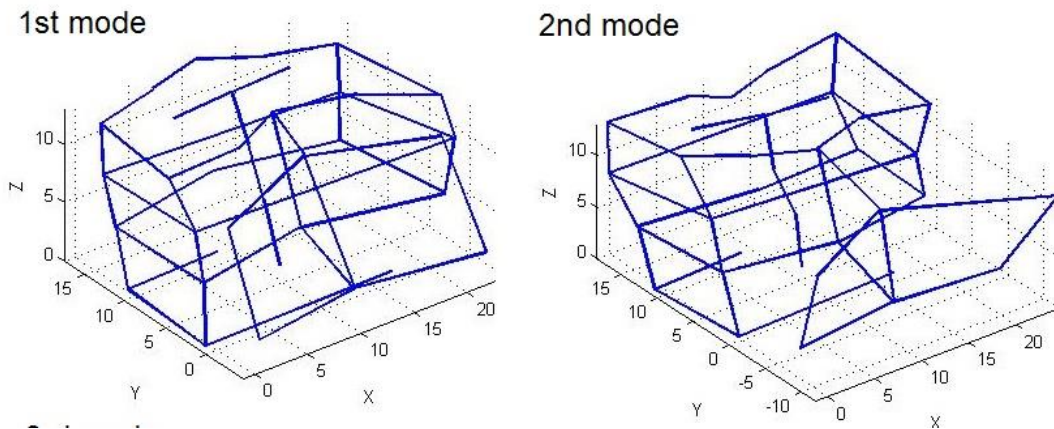


Figure 47: Mode shapes identified from the ambient vibration testing data

The combined stochastic subspace method was applied to the post-processed field forced vibration testing data to identify the modal characteristics of the structure. The Table 5 list the first 5 identified natural frequencies and damping ratios and the Figure 48 show the first 2 identified mode shapes.

Vibrational mode	Natural Frequency [Hz]	Damping ratio [%]
1	2.92	6.13
2	4.19	2.42
3	5.31	3.87
4	6.59	5.10
5	9.40	2.40

Table 5: Natural frequencies and damping ratios of the structure from the forced vibration testing data

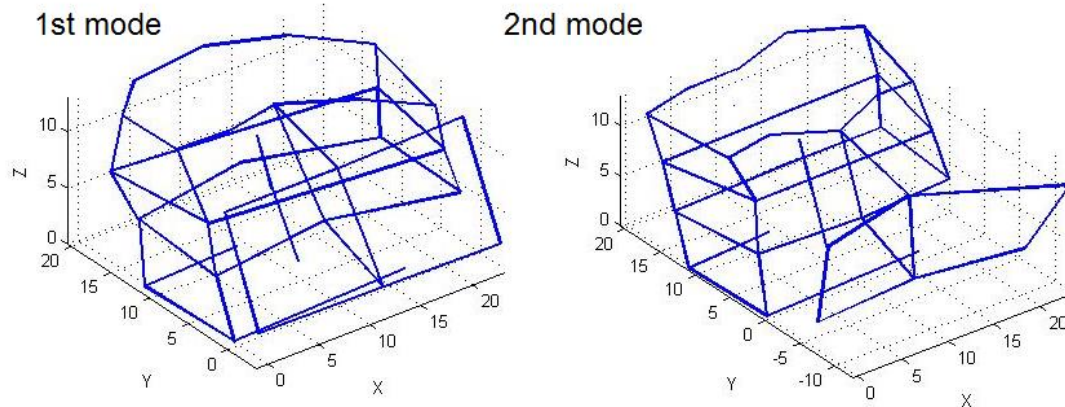


Figure 48: Mode shapes identified from the forced vibration testing data

From the results of the modal analysis of the field testing data it is interesting to notice that in the range 0-10 Hz it is possible to identify one vibrational mode more from the forced vibration testing data respect to the ambient vibration data. The values of the damping ratios corresponding to the common identified modes are different, and the mode shapes showed in the Figures 47 and 48 present minor differences.

10 References

- Boutin, C., Hans, S., Ibraim, E., & Roussillon, P. (2005). In situ experiments and seismic analysis of existing buildings - part II: seismic integrity threshold. *Earthquake engineering and structural dynamics*, 34(12), 1531-1546.
- Brownjohn, J. M., Pavic, A., & Reynolds, P. (2008). Advances in dynamic testing methods for in-situ civil engineering structures. *7th european conference in structural dynamics*, (S. E252). Southampton.
- Brüel & Kjaer. (kein Datum). *Brüel & Kjaer*. Von <http://www.bksv.it/>. abgerufen
- Bui, T. T., & De Roeck, G. (2012). Vulnerability assessment of structures in a lo-to-moderate seismic region based on ambient vibration test modal data. *11th International Conference on Computational Structures Technology*. Dubrovnik: Croatia.
- Cantieni, R. (2004). experimental methods used in system identification of civil engineering structures. *2° Workshop in "Problemi di vibrazioni nelle strutture civili e nelle costruzioni meccaniche"*. Perugia, Italy.
- Celebi, M., & Crouse, C. B. (2001). *Recommendations for soil structure interaction (SSI)*. Emeryville, USA: COSMOS.
- Chopra, A. (2007). *Dynamics of Structures. Theory and Application to earthquake engineering - 3rd edition*. Prentice Hall.
- Clough, R. W., & Penzien, J. (1995). *Dynamics of structures - 3rd edition*. Berkeley, (USA): Computers Structures, Inc.
- Crocker, M. J. (2008). *Handbook of noise and vibration control*. Hoboken, NJ, USA: John Wiley & Sons.

- Cuhna, A., & Caetano, E. (2006). Experimental modal analysis of civil engineering structures. *Sound and vibration*, 6, 12-20.
- de Silva, C. W. (2005). *Vibration and shock handbook*. Taylor and Francis.
- Dorf, R. C. (2000). *Dynamics and vibrations, the engineering handbook*. Boca Raton: CRC Press LLC.
- FEMA. (2003). *HAZUS-MH MR3 Technical Manual*.
- FEMA. (2003). *HAZUS-MN MR3 Technical Manual*.
- Flesch, R., Friedl, H., & Kwapisz, M. (2011). Nachweis der Erdbebensicherheit einer Verbrennungsanlage für radioaktive Abfälle. 12. D-A-C-H Tagung 2011 - Erdbeben und Baudynamik, Deutsche Gesellschaft für Erdbebeningenieurwesen und Baudynamik (DGEB), (S. 387-398). Hannover (Germany).
- Gazetas, G. (1983). Analysis of machine foundation vibrations: state of the art. *Soil dynamics and earthquake engineering*, 2(1), 2-42.
- Harris, C. M., & Piersol, A. G. (2002). *Harris' shock and vibration handbook*,. New York: McGraw Hill.
- Lang, G. F. (April 1997). Electrodynamic shaker fundamentals. *Sound and vibration*, S. 1-8.
- Lang, G. F., & Snyder, D. (October 2008). Understanding the physics of electrodynamic shaker performance. *Sound and vibration*, S. 1-9.
- LDS DACTRON. (kein Datum). Basics of structural vibration testing and analysis. *Application note ano11*.
- Michel, C., Gueguen, P., & Causse, M. (2012). Seismic vulnerability assessment to slight damage based on experimental modal parameters. *Earthquake engineering and structural dynamics*, 41(1), 81-98.
- Mistler, M., & Heiland, D. (2009). Artificial excitation methods for dynamic tests in buildings. *EVACES '09: Experimental vibration analysis for civil engineering structures*, (S. 189-200). Wroclaw (Poland).
- nees@ucla. (kein Datum). <http://nees.ucla.edu/>. Von nees@ucla. abgerufen
- Pavic, A., Pimentel, C., & Waldron, P. (1998). Instrumented sledge hammer excitation: worked examples. *IMAC XVI - 16th International Modal Analysis Conference - Model Updating & Correlation*, (S. 929-935). Santa Barbara, Ca, US.
- Peeters, B., & De Roeck, G. (1999). Reference-based stochastic subspace identification for output-only modal analysis. *Mechanical systems and signal processing*, 13(6), 855-878.
- Peeters, B., Maeck, J., & De Roeck, G. (2000). Excitation sources and dynamic system identification in civil engineering. *European COST F3 Conference on system identification and structural health monitoring*, (S. 341-350). Madrid (Spain).
- Raptakis, D., Chávez-García, F. J., Makra, K., & Pitilakis, K. (2000). Site effects at Euroseistest-I. Determination of the valley structure and confrontation of observations with 1D analysis. *Soil dynamics and earthquake engineering*, 19(1), 1-22.
- Reynders, E., & De Roeck, G. (2008). Reference-based combined deterministic-stochastic subspace identification for experimental and operational modal analysis. *Mechanical systems and signal processing*, 22(3), 617-637.
- Reynders, E., Houbrechts, J., & De Roeck, G. (2001). Automated interpretation of stabilization diagrams. *29th International Modal Analysis Conference Series, Modal analysis topics*, 3, S. 189-201. Jacksonville, USA.
- Reynders, E., Houbrechts, J., & De Roeck, G. (2012). Fully automated (operational) modal analysis. *Mechanical systems and signal processing*, 29, 228-250.

- Reynders, E., Pintelon, R., & De Roeck, G. (2008). Uncertainty bounds on modal parameters obtained from Stochastic Subspace Identification. *Mechanical systems and signal processing*, 22(4), 948-969.
- Reynders, E., Schevenels, M., & De Roeck, G. (2011). *MACEC 3.2: a Matlab toolbox for experimental and operational modal analysis, user's manual, Report BWM*. Leuven: K.U. Leuven.
- Shih, C. Y., Tsuei, Y. G., Allemang, R. J., & Brown, D. (1988). Complex mode indicator function and its applications to spatial domain parameter estimation. *Mechanical systems and signal processing*, 2(4), 367-377.
- Stokoe, K. H., Menq, F.-Y., Wood, S. L., Rosenblad, B. L., Park, K., & Cox, B. R. (2008). Experience with nees@UTexas large-scale mobile shakers in earthquake engineering studies. *3rd International Conference on Site Characteristic*, (S. 6pp). Taipei (Taiwan).
- Underwood, M. A., & Keller, T. (2008). Some application for the testing of civil structures using multiple shaker excitation techniques. *IMAC XXVI*. Orlando, USA.
- wilcoxon. (kein Datum). *wilcoxon*. Von <http://www.wilcoxon.com/>. abgerufen

Appendix: MoSeS: the AIT's MOBILE SEismic Simulator

The AIT's MOBILE SEismic Simulator is an electrohydraulic shaker mounted on a truck and is self-contained power generator. This shaker was developed considering the long experience gained during the extensive use of reaction mass exciters and another electro-hydraulic shaker (see case of study one).

The AIT's MOSES can be used as shaker working in 45° angle or as reaction mass working in horizontal or vertical direction. It generates signal varying in the range 0-80 Hz, with the possibility to use continuous frequency sweeps or variable sweep velocity.

The excitation force generated depends on the mass loading. It has three different mass loading configurations:

- 201 Kg when it is used without mass plates,
- 830 Kg when it is used with 2 mass plates and
- 1432 Kg when it is used with 4 mass plates.

The force is constant at 15 kN from approximately 3 Hz for full mass loading. The maximum force of 25 kN is constant starting from 7 Hz.

The hydraulic piston has a stroke of 250 mm, velocity of 0.56 m/s and force of 25kN.

The main differences compared to usual reaction mass exciter is, that no additional guide fillets like linear bearings are used. This is the main disadvantage of comparable exciter technologies, because it causes failure under high dynamic loading. This problem was overcome by guiding the mass only by a cylinder equipped with piston ducts on both its sides. These piston ducts are located one at the top of the piston and one at its bottom. The piston movement is controlled by an integrated displacement sensor. The ducts of the piston are bolted to double frame to which the additional mass plates are fixed. When the additional mass plates are not used, they are fastened to an external frame connected with the shaker

support. For this reason MOSES is always fully equipped and its can be used with different configuration during the same measurement campaign.

The excitation force is measured by the three load cells at the base of the moving part of the shaker when it is used as reaction mass in vertical direction or at the top of the ma the moving mass when the shaker is used as reaction mass in horizontal direction. The excitation force is recorded at the end of the rod chain by means of a strain gauge when the shaker is used in a 45° angle.

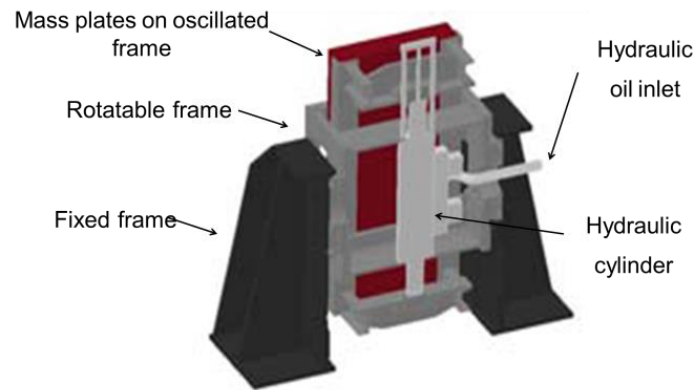


Figure 49: MoSeS' schema.

The AIT electro-hydraulic shaker is mounted on a modified two axes truck that is 7 m long, 3.7 m large and weights 134 kN. The shaker is fastened to the platform of this truck for the transport and it is loaded up and down from the platform by a skip loader. The van body stores the shaker hydraulic unit. The fluid is pumped in the shaker flow through a flexible tube fixed on the truck. The truck has a compartment on the bottom where both the power units of the hydraulic system and the skip loader are located. These power units are fuelled by an on-board tank: this makes the AIT's MOSES self-contained power generator. It can be used anyway also with an external electric supply.



(a)



(b)



(c)

Figure 50: Electrohydraulic exciter and truck (a). Power unit (b). Pressure accumulator (c).

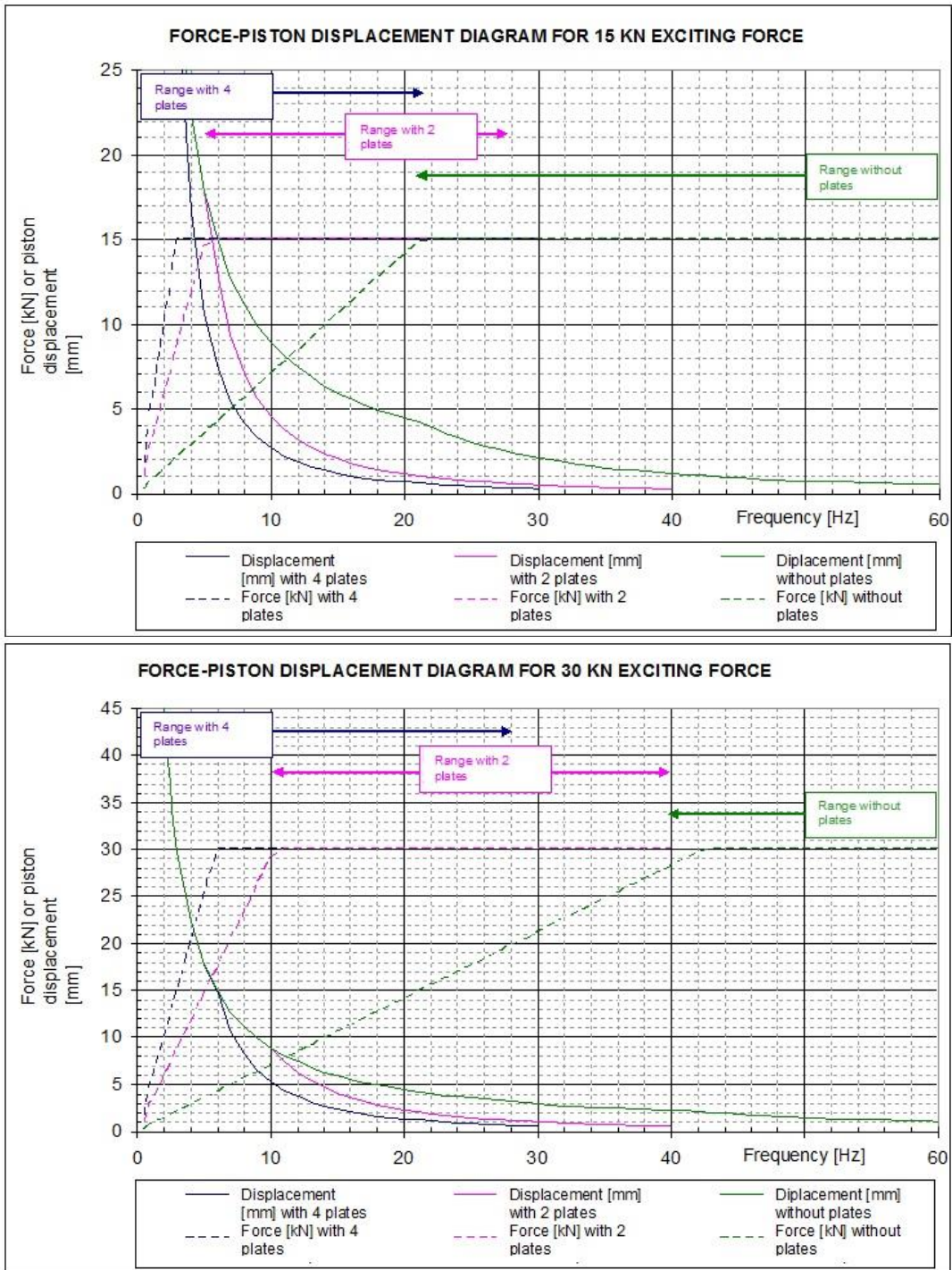


Figure 51: Diagrams of force-piston displacement for different frequency ranges and loads (0, 2 or 4 plates).